Annu. Rev. Phys. Chem. 1998. 49:125–71

CHEMICAL REACTION DYNAMICS BEYOND THE BORN-OPPENHEIMER APPROXIMATION

Laurie J. Butler
Department of Chemistry and The James Franck Institute, The University of Chicago, Chicago, Illinois 60637; e-mail: ljb4@midway.uchicago.edu

KEY WORDS: chemical reaction dynamics, transition state theory, nonadiabatic, potential energy surfaces, photodissociation

ABSTRACT

To predict the branching between energetically allowed product channels, chemists often rely on statistical transition state theories or exact quantum scattering calculations on a single adiabatic potential energy surface. The potential energy surface gives the energetic barriers to each chemical reaction and allows prediction of the reaction rates. Yet, chemical reactions evolve on a single potential energy surface only if, in simple terms, the electronic wavefunction can evolve from the reactant electronic configuration to the product electronic configuration on a time scale that is fast compared to the nuclear dynamics through the transition state. The experiments reviewed here investigate how the breakdown of the Born-Oppenheimer approximation at a barrier along an adiabatic reaction coordinate can alter the dynamics of and the expected branching between molecular dissociation pathways. The work reviewed focuses on three questions that have come to the forefront with recent theory and experiments: Which classes of chemical reactions evidence dramatic nonadiabatic behavior that influences the branching between energetically allowed reaction pathways? How do the intramolecular distance and orientation between the electronic orbitals involved influence the nonadiabaticity in the reaction? How can the detailed nuclear dynamics mediate the effective nonadiabatic coupling encountered in a chemical reaction?

0066-426X/98/1001-0125$08.00

INTRODUCTION

Much of the predictive ability for the branching between chemical reaction pathways has relied on statistical transition state theories (1–3) or, in smaller systems, quantum scattering calculations (4–9) on a single adiabatic potential energy surface. The potential energy surface gives the energetic barriers to each chemical reaction and allows prediction of the reaction rates. Yet the chemical reaction dynamics evolves on a single potential energy surface only if the Born-Oppenheimer (10) separation of nuclear and electronic motion is valid. The experiments and associated theory reviewed here seek to identify what classes of chemical reactions are particularly susceptible to a breakdown of the Born-Oppenheimer or electronic adiabatic approximation and to show how such a breakdown can markedly change the competition between energetically allowed chemical bond fission or molecular elimination pathways. Although I focus on photodissociation experiments here, the findings are equally important for bimolecular reactions in the ground electronic state. In both cases, the required change in the electronic wavefunction on traversing the reaction barrier can result in the failure of the common assumption that the reaction dynamics evolves on a single potential energy surface.

HISTORICAL BACKGROUND

Fundamental theories of the rates of elementary chemical reactions often begin by depicting a chemical reaction coordinate where the collision between two reactant molecules (or, in the case of photodissociation, the absorption of a photon) allows the system to surmount an energetic barrier along the reaction coordinate and then go on to products. The potential energy along the reaction coordinate is determined from a cut through the multidimensional potential energy surface for the reaction, which is calculated by freezing the internuclear distances at each geometry and solving the electronic part of the Schrödinger equation. If one then goes on to predict the reaction rate by using the usual transition state theories (1, 2) or by solving the "exact" nuclear dynamics using a Hamiltonian with only this potential energy and the nuclear kinetic energy, then one has implicitly assumed that the electronic wavefunction can instantaneously adjust as molecular bonds stretch, break, and form. This implicit assumption, the electronically adiabatic or Born-Oppenheimer approximation, was recognized and briefly challenged even at the inception of transition state theory. The originators of transition state theory, Evans and Polyani, briefly mentioned the adiabatic assumption (11) and, in a later Faraday discussion of a paper by the same authors (12), E Rabinowitch challenged that assumption. In the following paper (13), E Wigner also discusses the complex implications of

the electronic adiabatic assumption implicit in transition state theories. However, perhaps because of the early success of transition state theories and the later focus on another key assumption in transition state theory, that of intramolecular vibrational energy redistribution, the pitfalls in the implicit use of the Born-Oppenheimer approximation to understand chemical reaction rates have been largely overlooked. Thus, although it was challenged at the inception of transition state theory, the adiabatic approximation is often now implicitly assumed to be valid for bimolecular and unimolecular reactions in the ground electronic state (2, 4, 5). Its shortcomings are only widely recognized for ion-molecule, charge transfer (14), and other reactions involving obvious electronic curve crossings (15, 16). One of the best prior reviews (17) of nonadiabatic molecular collisions, one that primarily focuses on theoretical methods, does indeed note that not only reactions involving electronically excited species and ion-molecule reactions can be nonadiabatic, but also reactions of ground state species at room temperature. The experiments reviewed here seek to demonstrate the importance of considering the possibility of nonadiabaticity at the transition state of any chemical reaction with a barrier along the reaction coordinate, including ground-state bimolecular reactions, and to identify the classes of chemical reactions in which nonadiabatic effects are most critical. To understand the rates of chemical reactions in terms of statistical transition state models, the experiments provide compelling evidence that the failure of the adiabatic approximation can be as important as the more thoroughly scrutinized (18–21) assumption of intramolecular vibrational energy redistribution in predicting the rates of, and thus competition between, chemical reaction channels.

This review focuses on experimental work primarily from my own research group, with only passing mention of other work in the area of electronically nonadiabatic chemical reactions. Although this review describes some theoretical work associated with the experiments reviewed, it does not attempt to review the wealth of theoretical advances in the area of electronically nonadiabatic reaction dynamics. For this, I refer the reader to a number of review articles by theoreticians on nonadiabatic processes (22–34); a beginner with an experimental tilt can start with the previously mentioned review by Tully (17) or the 1981 review by Garrett & Truhlar (26). The experiments reviewed below primarily focus on nonadiabatic interactions that arise from radial derivative coupling, the coupling that results from the change in electronic wavefunction with changing internuclear separations, rather than nonadiabatic coupling that derives from the rotation of the entire molecular system (such as Coriolis coupling). I also follow the convention noted by Tully (17) that the term "adiabatic" representation, which has been used for eigenfunctions and eigenvalues of either $\mathcal{H}_o = \mathcal{H}_{el} + \mathcal{H}_{SO}$ [see Tully (17) for definitions] or for only

$\mathcal{H}_{el}$ depending on the context, is used for the eigenfunctions and eigenvalues of $\mathcal{H}_{el}$ alone unless otherwise noted (thus assuming that spin orbit interactions are not important in the particular dynamics being discussed). I further restrict this review to electronic nonadiabatic effects in chemical reactions; the influence of electronic nonadiabaticity on bound states in molecular spectroscopy can also be considerable, as detailed in several reviews (35–39). Finally, whenever there is a conical intersection involved in the dynamics, one should also account for geometric phase (40) in the Hamiltonian in the adiabatic representation; because neither this review nor the Tully review addresses this point adequately, I refer the reader to previous reviews on geometric phase (41–44) and a beautiful recent review by Yarkony (22).

This review starts with a qualitative pedagogical description of electronically nonadiabatic effects to demonstrate first why the Born-Oppenheimer approximation is particularly subject to breakdown near the transition state of a chemical reaction, and then how, in a simple two-state model, the breakdown results in reducing the chemical reaction rate. The next section shows that such a breakdown can dramatically change the branching ratios between two energetically allowed reaction channels, detailing experiments wherein the reaction channel with the higher energy barrier totally dominated another channel with a 10 kcal/mole lower energy barrier! The review continues with a more specialized treatment of the subject, (*a*) exploring what classes of chemical reactions are particularly subject to nonadiabatic effects, (*b*) investigating the influence of molecular conformation and intramolecular separation on electronic nonadiabaticity, (*c*) examining experiments that access the transition state to probe nonadiabatic effects, and (*d*) detailing the influence of the multidimensional nature of the reactive potential energy surface and how it can mediate electronically nonadiabatic effects in both ground state and excited state chemical reactions. Throughout the article, I try to acknowledge the pioneers in electronic structure theory who have performed difficult calculations to obtain derivative coupling matrix elements in addition to multidimensional potential energy surfaces; the lack of derivative coupling matrix elements is perhaps the leading reason why "exact" quantum scattering calculations often neglect to include important nonadiabatic effects.

WHY THE BORN-OPPENHEIMER APPROXIMATION CAN BREAK DOWN AT THE TRANSITION STATE OF A CHEMICAL REACTION

This section seeks to give a clear physical picture of the particular susceptibility of the Born-Oppenheimer approximation to breakdown at a point that is crucial for chemistry—at the transition state of a chemical reaction. I begin with some

mathematical formalism and then analyze the change in electronic wavefunction required for a molecule to remain on one potential energy surface as it tries to cross the barrier to a chemical reaction. I show that the change in electronic wavefunction required to cross the transition state is sometimes so large that it renders invalid the Born-Oppenheimer approximation, which assumes that the electronic wavefunction can readjust instantaneously on the time scale of nuclear motion.

Tully (17) gives an excellent review of nonadiabatic interactions, including the particular terms in the Schrödinger equation that one assumes are zero when it is presumed that the nuclear dynamics propagate on a single potential energy surface. Although in an adiabatic representation there are three such neglected terms (omitting geometric phase), one diagonal and two off-diagonal, Tully argues that the most important nonadiabatic coupling is provided by the off-diagonal terms $\mathcal{T}'_{kk'}(k \neq k')$

$$\mathcal{T}'_{kk'} = \sum_{M=1}^{N-1} -\left(\frac{\hbar^2}{2\mu_M}\right) \left\langle \varphi_k \middle| \vec{\nabla}_M \middle| \varphi_{k'} \right\rangle \cdot \vec{\nabla}_M \qquad 1.$$

where φ_k is the electronic eigenfunction at a particular point on the kth potential energy surface that one gets from the solution of the electronic part of the Schrödinger equation, and M indexes the particular internuclear coordinate (bond stretch, angle bend, torsion) or molecular rotation in the N atom system. Thus, this term can include both Coriolis coupling and internuclear coordinate derivative coupling (in diatomics, often termed "radial derivative coupling").

To understand why the Born-Oppenheimer approximation can break down near the transition state for a chemical reaction, consider $\langle \varphi_{k'} | \vec{\nabla}_M | \varphi_k \rangle$ for an M corresponding to motion along an internuclear coordinate that moves the system across the transition state. (This internuclear coordinate (or "radial") derivative coupling matrix element is the negative complex conjugate of the corresponding matrix element $\langle \varphi_k | \vec{\nabla}_M | \varphi_{k'} \rangle$ in the middle of the nonadiabatic coupling term given in Equation 1.) This matrix element gets large near the transition state for a chemical reaction, rendering the Born-Oppenheimer approximation suspect. This is easy to see. The matrix element $\langle \varphi_{k'} | \vec{\nabla}_M | \varphi_k \rangle$ involves the change of the electronic eigenfunction φ_k of the potential surface k on which the nuclear dynamics is trying to propagate. If the nuclear coordinate is a bond stretch in a diatomic, then the expression involves $\nabla_R \varphi_k = \frac{\partial}{\partial R} \varphi_k$. Take the case where the change in internuclear coordinate R moves along the reaction coordinate of the chemical reaction. The change in electronic eigenfunction across the transition state is typically large, as evidenced in the following example of the excited state $H + SH \rightarrow H + SH$ reaction depicted in Figure 1 (45). The figure shows the highest occupied molecular orbital (HOMO) of the electronic eigenfunction

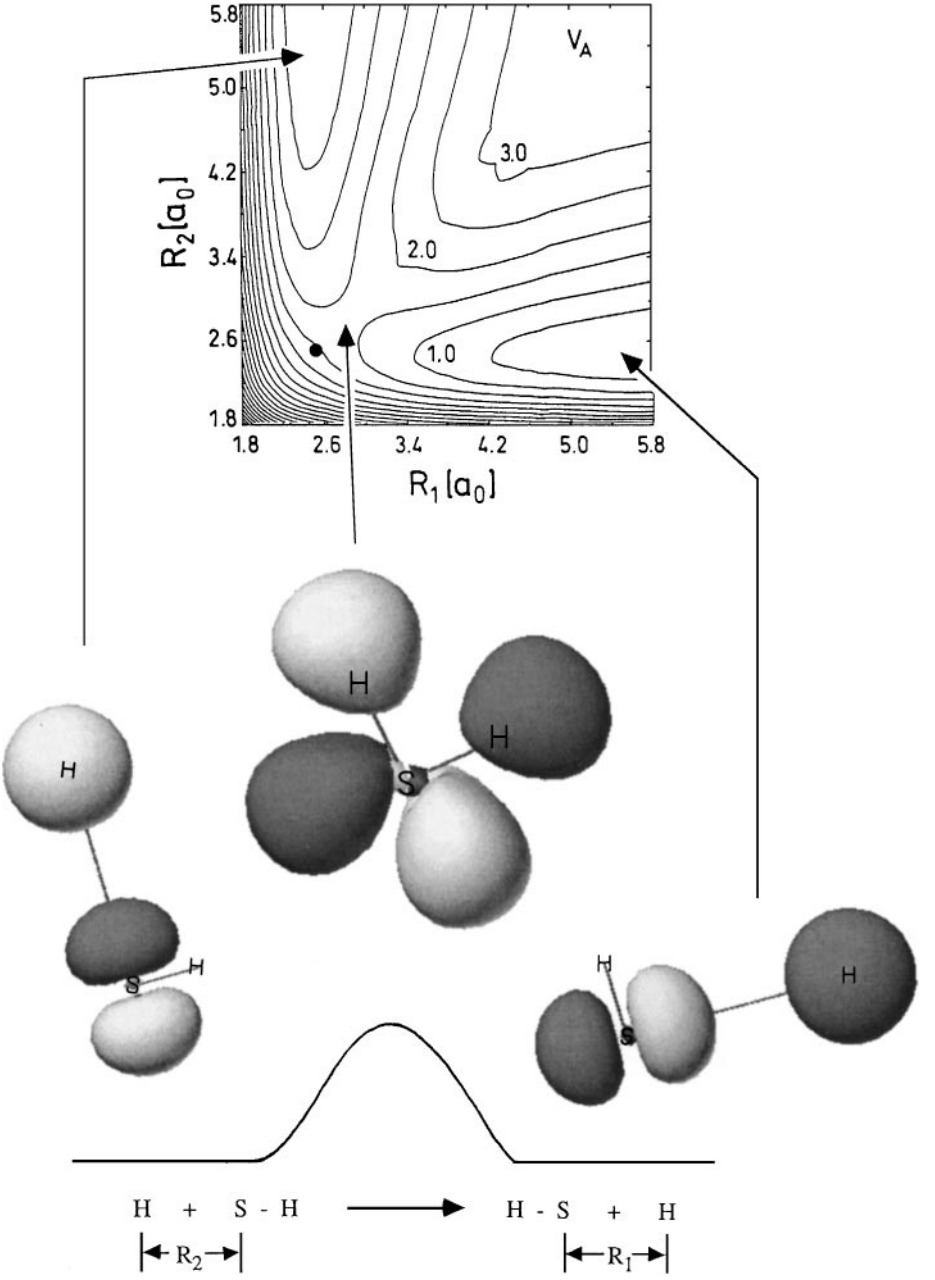
5.8
5.0
4.2
3.4
2.6
1.8
$R_2[a_0]$
V_A
3.0
2.0
1.0
1.8
2.6
3.4
4.2
5.0
5.8
$R_1[a_0]$
H
H
S
H
S
H
H
S
H
H + S - H
H - S + H
R_2
R_1

on the HSH excited state potential energy surface. In the entrance channel, the wavefunction has localized antibonding character between the incoming hydrogen and the S of the SH reactant; this antibonding interaction is why the potential energy surface goes uphill as the H atom approaches the SH (or as R_2 in the figure decreases). At the transition state, the HOMO looks much different, and in the exit channel, it now looks antibonding between the HS and the exiting H atom, consistent with the downward slope of the potential energy surface after the transition state as R_1 lengthens. Thus, the electronic wavefunction changes markedly as the dynamics traverses the reaction barrier, from antibonding between the incoming H atom and the S atom before the transition state to antibonding in the other SH bond after the transition state. The term $\nabla_R \varphi_k = \frac{\partial}{\partial R}\varphi_k$ is large near $R_1 = R_2$, and thus the matrix element in Equation 1 for $\mathcal{T}'_{kk'}$ becomes large near the transition state, potentially rendering the Born-Oppenheimer approximation invalid because the approximation assumes $\langle \chi_k | \mathcal{T}'_{kk'} | \chi_{k'} \rangle$ is negligible. Physically, the change in electronic wavefunction required for the nuclear dynamics to continue to propagate only on the given potential energy surface is too large unless the relative nuclear velocity is small (the matrix element is velocity dependent in this semiclassical sense because $\mathcal{T}'_{kk'}$ operates on $\chi_{k'}$, so it involves $\vec{\nabla}_M$ operating on the nuclear wavefunction).

REDUCTION IN THE RATE OF A CHEMICAL REACTION FROM NONADIABATIC RECROSSING OF THE REACTION BARRIER

The inability of the electronic wavefunction to change with nuclear motion as the dynamics attempts to traverse the transition state can simply result in a dramatic reduction in the rate constant for the chemical reaction. The qualitative mechanism for such a reduction in a reaction rate because of nonadiabatic recrossing of a barrier is illustrated in Figure 2 for an A-B bond fission reaction with a barrier along the forward and reverse reaction coordinates.

←

Figure 1 Schematic reaction coordinate and Born-Oppenheimer potential energy surfaces for the excited state reaction $H + SH \rightarrow HS + H$. The change in electronic wavefunction required to follow the adiabatic reaction coordinate as one traverses the transition state region is shown by depicting the highest occupied valence molecular orbital in the entrance channel (*left*), at the transition state (*middle*) and in the exit channel (*right*). (For pedagogical clarity, I have deleted the Rydberg character also present in the actual H_2S system.) One can see that the electronic wavefunction at the transition state is a linear combination of the reactant and product electronic configurations. Upper portion adapted with permission from Figure 2 of Reference 97 (copyright 1994, American Institute of Physics). Lower portion (orbitals) adapted with permission from Figure 5 of Reference 98 (copyright 1994, American Institute of Physics).

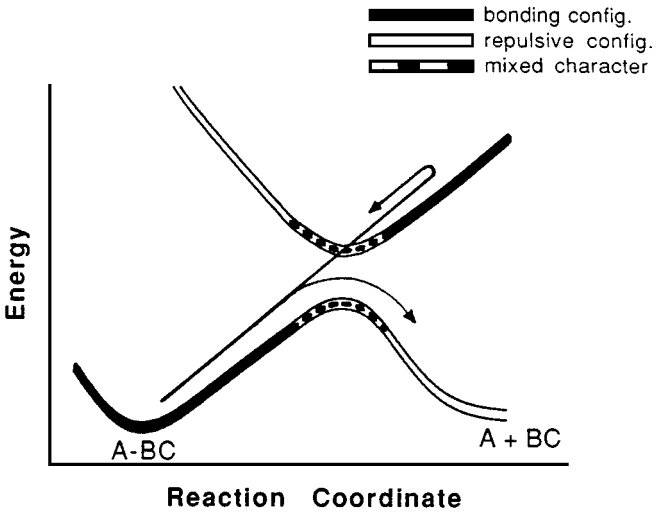

Figure 2 Schematic depiction of nonadiabatic recrossing of the transition state of a bond fission reaction where on the lower adiabat the electronic wavefunction must change from bonding to mixed to antibonding in character. In this simple two-state model, the lower and upper adiabats are formed from the avoided electronic configuration crossing of a bonding electronic configuration and a repulsive electronic configuration. If the Born-Oppenheimer approximation fails, the molecule retains its bonding electronic character at the barrier and makes a non-adiabatic "hop" to the upper adiabat instead of proceeding to products on the lower adiabat. (Reproduced with permission from Figure 1 of Reference 59, copyright 1994, American Institute of Physics.)

Along the adiabatic reaction coordinate, the dominant electronic configuration changes from bonding in the A-B bond, on the reactant side of the barrier, to repulsive in the A-B bond, after the barrier in the exit channel region. In a simple two-state model, one can view any adiabatic reaction coordinate with a saddle point at the transition state as being formed from such an avoided electronic configuration crossing [this is as true for saddles on the ground state potential energy surface as it is for excited state potential energy surfaces (15, 16, 46, 47)]. The change in electronic wavefunction required to follow the adiabatic reaction coordinate near the barrier is considerable and can result in a failure of the Born-Oppenheimer approximation. If the splitting between the adiabatic electronic surfaces at the barrier along the reaction coordinate is small (48) reflecting the weak configuration interaction between the bonding and repulsive electronic configurations, the molecule may not traverse the barrier adiabatically. Instead the electronic wavefunction may retain the character of the bonding configuration, resulting in a nonadiabatic hop to the upper, bound potential energy surface at the avoided crossing. The molecule feels the bound wall of that potential instead of undergoing bond fission on the lower adiabat.

Several classes of reactions are susceptible to a reduction in the rate constant from nonadiabatic recrossing of the reaction barrier. A completely analogous mechanism to that described above results in a nonadiabatic reduction in the rate constant for electron transfer reactions (14). In a statistical expression for the reaction rate constant $k = \kappa(k_B T/h)\frac{q^{\ddagger}}{q_A q_B} \exp(-E_o/k_B T)$, one may correct for this recrossing with a transmission factor κ of less than one (14, 49).[1] [Traditionally, however, a reduced κ has been used to correct for recrossing that results from a large curvature of the potential energy surface in the transition state region, not for recrossing that results from nonadiabatic transitions (50).] The work reviewed in the next two sections shows that the reduction in rate resulting from nonadiabatic recrossing of the barrier can markedly change the branching between competing bond fission pathways and identifies two classes of reactions in which such nonadiabatic effects play a dominant role in product branching.

HOW NONADIABATIC RECROSSING CAN ALTER THE BRANCHING BETWEEN TWO COMPETING BOND FISSION REACTIONS

Competing C-Br and C-Cl fission in Bromoacetyl Chloride

The first experiment reviewed here provides a compelling reason to reexamine the common practice of predicting reaction rates for competing chemical reactions based on the relative barrier heights along the two reaction coordinates. The common wisdom is that given similar preexponential factors, the reaction channel with the lower energy barrier has a faster rate constant compared to a reaction channel with a higher energy barrier. The first excited singlet state of bromoacetyl chloride is an A'' state with a barrier to C-Br fission that is roughly 10 kcal/mole lower than the barrier to C-Cl fission. Since the A factor is expected to be similar for these two bond fission channels, one would expect C-Br fission to dominate C-Cl fission upon photoexcitation to the A'' potential energy surface. Crossed laser-molecular beam experiments (51–53) however, show that the reverse occurs; C-Cl fission, the channel with the higher barrier, dominates C-Br fission by a ratio of 1.0:0.4. [The excitation wavelength of 248 nm is in an overlapping region of the absorption spectrum where most of the molecules are excited via the $n_O \pi^*_{C=O}$ transition to the $1A''$ potential energy surface, but some are excited to a surface that is diabatically repulsive in the C-Br bond; thus, the branching ratios given are the result of subtracting from the data the C-Br bond fission events from direct excitation to the overlapping repulsive state.] The analysis of that work, described below, is proposed with a

[1]Evans & Evans (49) first corrected a bimolecular reaction rate for adiabatic versus diabatic crossing. They used Landau-Zener theory for the now well-recognized case of a reaction involving the crossing of ionic and covalent electronic states.

leap of intuition, that C-Br fission is suppressed in bromoacetyl chloride by the inability of the electronic wavefunction to "keep up" with the C-Br stretching across the barrier to C-Br fission on the $1A''$ potential energy surface. The model suggests that nonadiabatic recrossing (see previous section) of the C-Br fission reaction barrier suppresses the rate of that reaction channel, allowing the higher energy C-Cl fission channel to compete effectively. I describe the model in detail below, along with subsequent work that tests the nonadiabatic recrossing hypothesis with an experiment on the branching between C-Br fission and C-Cl fission in bromopropionyl chloride.

Nonadiabatic Recrossing of the C-Br Fission Transition State

To understand the proposed model for nonadiabatic suppression of the C-Br fission rate constant, first consider how the electronic wavefunction must change along the C-Br fission reaction coordinate on the $1A''$ potential energy surface.[2] In the reactant region accessed in the Franck-Condon region, the electronic wavefunction clearly looks $n_O\pi^*_{C=O}$ in character; in a natural orbital description the $\sigma^*_{C\text{-}Br}$ orbital is unoccupied, and there are two sigma bonding electrons on the C-Br bond. A qualitative configuration interaction with single excitations (CIS) electronic structure calculation (45) shows, as expected, that the adiabatic Born-Oppenheimer potential energy surface goes uphill as the C-Br bond is stretched, reflecting the bonding character of the electronic wavefunction on the C-Br bond. However, after the transition state, the electronic wavefunction on the $^1A''$ potential energy surface has changed dramatically. It now looks $n_{Br}\sigma^*_{C\text{-}Br}$ in character, and the potential energy surface shown in Figure 3 (*top*) is repulsive in the C-Br bond after the transition state. Within the Born-Oppenheimer approximation, by neglecting the term $\langle\chi_k|\mathcal{T}'_{kk'}|\chi_{k'}\rangle$, one makes the approximation that the nuclear dynamics propagates on this single potential energy surface, that the electronic wavefunction readjusts to the repulsive electronic configuration as the nuclear dynamics crosses the transition state. In the proposed model explaining the suppression of C-Br fission, it was suggested that the electronic wavefunction did not readjust, that the molecule retained $n_O\pi^*_{C=O}$ character through the transition state. In that case, the effective potential energy that the nuclear dynamics feels is one determined by an $n_O\pi^*_{C=O}$ configuration at C-Br distances past the transition state, a configuration bound,

[2]Throughout this discussion I will consider the spatial character of the electronic wavefunction only, neglecting consideration of spin. Although this will obviously not yield quantitative results in a system where spin-orbit coupling is strong, the argument still retains the essential physical characteristics of the dynamics. The $n\sigma^*$ repulsive electronic configurations characteristic of a C-Br moiety will thus be crudely referred to here as $^1A'$ and $^1A''$ in symmetry, where in fact the singlet and triplet configurations mix strongly and produce five repulsive spin-orbit states.

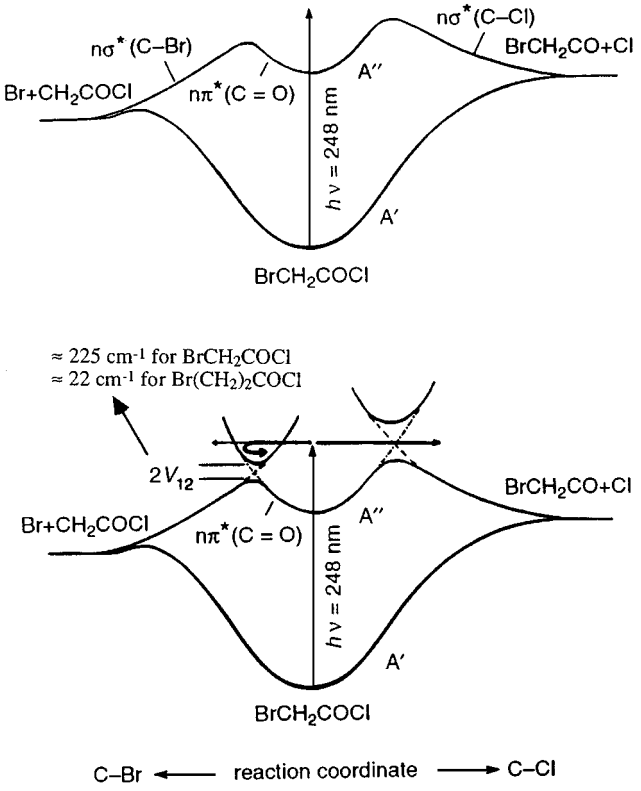

Figure 3 Schematic reaction coordinates for C-Cl and C-Br fission from the 248 nm photodissociation of $Br(CH_2)_nCOCl$. The lower frame shows the splitting, determined from configuration interaction with single excitations calculations at $r_{C=O} = 1.188$ Å (for $BrCH_2COCl$) and $r_{C=O} = 1.195$ Å (for $Br(CH_2)_2COCl$), between the two A'' potential energy surfaces at the avoided crossing along the C-Br bond fission coordinate. (Adapted with permission from Figures 1 and 11 of Reference 57, copyright 1993, American Institute of Physics.)

not repulsive, in the C-Br bond. This is a higher energy electronic configuration at stretched C-Br distances compared to the $n_{Br}\sigma^*_{C\text{-}Br}$ electronic configuration that characterizes the $1^1A''$ potential energy surface after the transition state, so the molecular dynamics has effectively undergone a "nonadiabatic hop" to the bonding region of the upper adiabatic $2^1A''$ potential energy surface, shown in Figure 3 (*bottom*). Trajectories, which would have had enough energy to surmount the C-Br fission reaction barrier and go on to products, instead sample the outer turning point of that bound upper adiabatic potential and turn back toward the reactant region. Another nonadiabatic hop as the C-Br bond

shortens, resulting from the electronic wavefunction again retaining $n_O\pi^*_{C=O}$ character, returns the nuclear dynamics back to the bonding region of the $1^1A''$ potential energy surface. The result is that a nuclear trajectory that should have resulted in C-Br fission does not, because the electronic wavefunction never readjusted enough for the nuclei to feel the repulsive potential that characterizes the reactive potential energy surface past the transition state. C-Br fission is effectively suppressed.

Adiabatic vs. Diabatic Representations: $\mathcal{T}'_{kk'}$ vs V_{12}

To test whether nonadiabatic recrossing of the transition state is the cause of the anomalously small yield of C-Br fission, it is helpful to understand the phenomena in both the above adiabatic representation and in a crude diabatic representation. The adiabatic representation is defined *always* by diagonalizing the electronic part of the Schrödinger equation so that the potential energy matrix $U_{kk'}$ in the nuclear part of the Schrödinger equation has no off-diagonal elements (e.g. in a two-state model, $U_{11}(R)$ and $U_{22}(R)$ are the lower and upper adiabatic potential energy surfaces and $U_{12} = U_{21} = 0$). The nonadiabatic hop is caused by the large $\langle \chi_k | \mathcal{T}'_{kk'} | \chi_{k'} \rangle$ matrix element (in the kinetic energy operator in the nuclear Hamiltonian) near the reaction barrier, because the electronic wavefunction changes so rapidly along the lower potential energy surface through the transition state. In a diabatic representation, one defines new potential energy surfaces V_{jj} where in a two-state model V_{11} is the potential energy associated at all nuclear geometries with a $n_O\pi^*_{C=O}$ bonding electronic configuration and V_{22} is the potential energy associated with a repulsive $n_{Br}\sigma^*_{C\text{-}Br}$ electronic configuration. Then the $\mathcal{T}'_{jj}$ term in this new diabatic representation is necessarily small, but since the $n_O\pi^*_{C=O}$ and $n_{Br}\sigma^*_{C\text{-}Br}$ configurations are not eigenfunctions of the electronic Hamiltonian, there are now significant (nonzero) off-diagonal terms V_{12} and V_{21} in the new potential energy matrix. The size of this off-diagonal potential coupling term determines whether the nuclear dynamics stays on the reactant diabatic potential energy surface characterized by the $n_O\pi^*_{C=O}$ bonding electronic configuration or crosses to the repulsive diabat characterized by the $n_{Br}\sigma^*_{C\text{-}Br}$ electronic configuration. If V_{12} is large, the nuclear trajectories have a large probability of crossing to the repulsive diabat and C-Br fission results. This transition at the diabatic "curve crossing" results in the normal *adiabatic* product channel. If V_{12} is small, the nuclear dynamics stays on the bound diabat, reaches the outer turning point of the bound potential along the C-Br stretch, and returns to the reactant region. Thus, a small off-diagonal potential coupling term in the diabatic representation results in the nuclear dynamics accessing the *bound* region of the higher of the two potential energy surfaces at stretched C-Br distances, just as a nonadiabatic hop from the $1^1A''$ to the $2^1A''$ potential energy surface does in the adiabatic representation. Small

off-diagonal potential coupling terms thus give rise to a large probability of a nonadiabatic hop in the adiabatic representation. In a two-state model, one may extract the magnitude of the off-diagonal potential coupling simply by looking at the energetic splitting between the two adiabats since $U_{22} - U_{11} = 2|V_{12}|$ at the avoided crossing.[3] In other words, if the energetic splitting $U_{22} - U_{11}$ between the two adiabats is very small near the transition state (one sometimes says the electronic configuration crossing is "narrowly avoided"), the corresponding off-diagonal potential coupling terms in the diabatic representation are small and the electronic wavefunction will retain its diabatic character as the nuclear dynamics tries to traverse the transition state. Thus, this two-state picture provides the simple result that a small energetic splitting between adiabats at the avoided crossing of the reaction barrier results in a large probability for reactive trajectories to nonadiabatically recross the transition state instead of proceeding to products. Such a small splitting reflects the small off-diagonal matrix elements in a diabatic representation.[4]

Modifying V_{12} to Test the Recrossing Model: Bromopropionyl Chloride

A way to test the proposed model presents itself. If the C-Br fission in bromoacetyl chloride is suppressed by nonadiabatic recrossing of the C-Br fission reaction barrier, one needs only to find a way to decrease the off-diagonal V_{12} matrix element still further, thus decreasing the energetic splitting between the

[3]The adiabats result from diagonalizing the matrix $\begin{pmatrix} V_{11} & V_{12} \\ V_{21} & V_{22} \end{pmatrix}$, so at the internuclear geometry R_{cross} where the diabats would have crossed $V_c = V_{11}(R_{cross}) = V_{22}(R_{cross})$ the diagonal elements U_{11} and U_{22} in the diagonalized matrix are then $U_{11} = V_c - |V_{12}|$ and $U_{22} = V_c + |V_{12}|$.

[4]This two-state model gives the intuitively understandable result that the electronic configuration interaction matrix element V_{12} is small if the splitting between the potential curves at the avoided crossing in the adiabatic representation is small. Additionally, the derivative coupling is large because the electronic wavefunction changes rapidly along the lower adiabat near the avoided crossing. However, this result is not a general one. Indeed, even if one diagonalizes a 3×3 matrix V_{ij} to get three potential surfaces, as in the case where three electronic configurations mix significantly and split to form the resulting adiabats, all off-diagonal potential couplings can be large but still result in potential surfaces in the adiabatic representation where two of the three adiabats come very close, or even intersect, each other. Such accidental intersections can thus occur between electronic states of the same symmetry as pointed out by Yarkony (54, 55). The reader may be convinced of this by diagonalizing the matrix $\begin{pmatrix} V_{11} & .1 & .3 \\ .1 & V_{22} & .2 \\ .3 & .2 & V_{33} \end{pmatrix}$, where the diabats are taken as $V_{11} = 2(2^{-R})$, $V_{22} = 8(R - .5)^2$, and $V_{33} = (R-1)^2 + Y$ at $R = 0.8641$ and $Y = 1.5$; changing only the value of Y, not the off-diagonal matrix elements, dramatically changes the splitting at avoided crossing between the lower two adiabats (B Zion, LJ Butler, unpublished information). If only two electronic configurations interact strongly, however, a large splitting between the resulting adiabats at the avoided crossing does imply that the configuration interaction matrix elements are small.

$1^1A''$ (U_{11}) and the $2^1A''$ (U_{22}) adiabats at the avoided crossing. If the model is correct, this should increase the nonadiabatic recrossing probability and thus suppress C-Br fission even more. It is easy to see from the expression in Equation 2 below that one can reduce V_{12}, and thus increase the nonadiabatic suppression of C-Br fission, by increasing the spatial separation between the C=O and C-Br orbitals.[5] The first matrix element below, similar to that in a Förster model for intramolecular electronic energy transfer, decreases with the separation between the C-Br and C=O orbitals because of the distance between the electrons, the r_{12}, in the denominator, while the second matrix element, similar to that in the Dexter energy transfer mechanism, decreases roughly exponentially as the overlap densities $n_O(1)n_{Br}(1)$ and $\pi^*_{C=O}(2)\sigma^*_{C\text{-}Br}(2)$ decrease.

$$V_{12} = 2\left\langle n_O(1)n_{Br}(2)\left|\frac{e^2}{r_{12}}\right|\pi^*_{C=O}(1)\sigma^*_{C\text{-}Br}(2)\right\rangle - \left\langle n_O(1)\pi^*_{C=O}(2)\left|\frac{e^2}{r_{12}}\right|n_{Br}(1)\sigma^*_{C\text{-}Br}(2)\right\rangle \quad 2.$$

Bromopropionyl chloride, with an additional CH_2 spacer between the C=O and C-Br orbitals, should thus show a further reduction in the low-energy C-Br fission channel. Subsequent crossed laser-molecular beam experiments showed just that (57). While in bromoacetyl chloride, the initial $^1(n_O\pi^*_{C=O})$ electronic transition resulted in a C-Cl:C-Br bond fission ratio of 1.0:0.4, in bromopropionyl chloride the same initial transition resulted in a C-Cl:C-Br bond fission ratio of 1.0:<0.05 (52, 57). The <0.05 branching to C-Br fission represents an upper limit; in fact, a comparison of the distributions of relative kinetic energies imparted to the C-Br fission fragments in the two molecules determined from the data in Figures 4 and 5 show that essentially all of the Br atom products observed from bromopropionyl chloride merely result from an overlapping transition to an electronic state diabatically repulsive in the C-Br bond. Figure 6 compares the kinetic energy distribution of the C-Br fission fragments from bromoacetyl chloride (*upper frame*), which evidences C-Br fission from both the $^1(n_O\pi^*_{C=O})$ transition and from the overlapping repulsive transition, with that from bromopropionyl chloride (*lower frame*). When one superimposes the component from bromoacetyl chloride for C-Br fission from just the overlapping transition, it corresponds closely to the entire distribution from bromopropionyl chloride as shown in Figure 6. Thus, the lower energy

[5]In these systems, identified below as Woodward-Hoffmann-forbidden reactions, the orthogonal basis evidences highly localized molecular orbitals because the one-electron exchange and resonance integrals calculated to orthogonalize the basis were already small; the switch in individual orbital symmetry thus results in anomalously small splittings for Woodward-Hoffmann forbidden reactions (56).

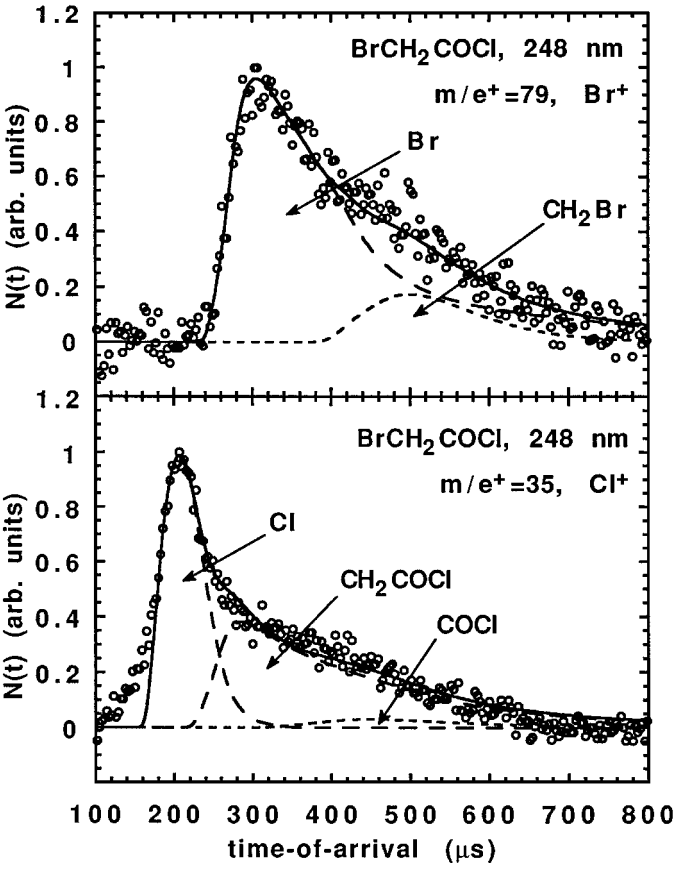

Figure 4 Laboratory time-of-flight data of the photofragments detected at Br^+ and Cl^+ from bromoacetyl chloride photodissociated at 248 nm with an unpolarized laser. The fits to the individual contributions are described in Reference 53. The forward convolution fit to the signal at Br^+ assigned to Br atoms, which dominates the fast side and peak of the spectrum, was obtained with the $P(E_T)$ for C-Br fission, shown in Figure 6 (*top*). (Reproduced with permission from Figure 2 of Reference 53, copyright 1994, American Institute of Physics.)

component from $^1(n_O\pi^*_{C=O})$ excitation is absent in bromopropionyl chloride; the higher energy C-Cl fission channel completely dominates C-Br fission on the $^1A''$ surface despite being the channel with the higher barrier. This further dramatic reduction in branching to C-Br fission upon $^1(n_O\pi^*_{C=O})$ excitation supports the hypothesis that the additional intervening CH_2 spacer would decrease the splitting between the adiabats at the avoided crossing and thus increase the nonadiabatic recrossing of the reaction barrier. A single reference configuration

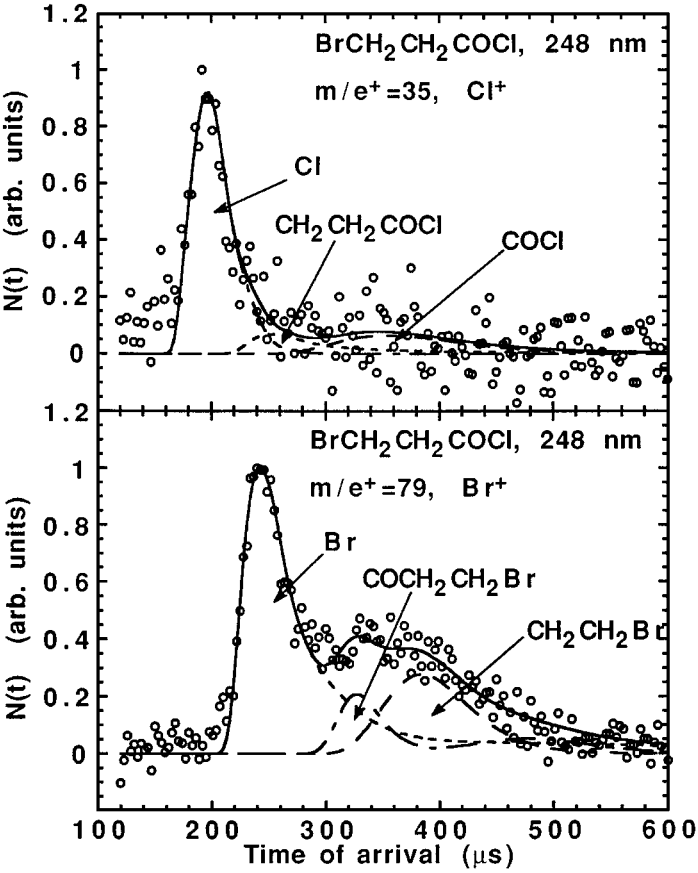

Figure 5 Laboratory time-of-flight data of the photofragments of bromopropionyl chloride detected at Cl^+ (*upper frame*) and Br^+ (*lower frame*) at 248 nm with an unpolarized laser. The source angle was 20° in the upper frame and 10° in the lower frame. The forward convolution fit to the portion of the signal at Br^+ assigned to Br atoms was obtained with the $P(E_T)$ for C-Br fission in Fig. 6 (*bottom*). (Reproduced with permission from Figure 3 of Reference 57, copyright 1993, American Institute of Physics.)

interaction (single excitations only) calculation (45) of the splitting between the adiabats at the barrier to C-Br fission in these two systems further tests this conclusion.While the approximations inherent in the method and the minimal (STO-3G*) basis set preclude quantitative accuracy, the results given in Reference 57 (57: Table 1) show that the splitting at the avoided crossing is an order of magnitude smaller in bromopropionyl chloride than in bromoacetyl chloride, consistent with the interpretation of the experimental results. The splitting in

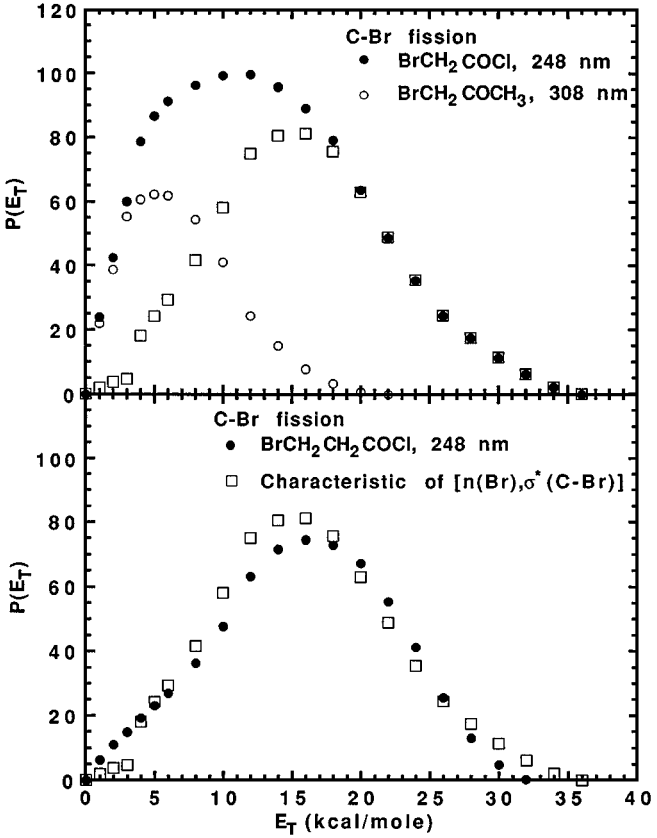

Figure 6 Center-of-mass product translational energy distributions, $P(E_T)$'s, from References 53 and 57, for the C-Br fission channel in bromoacetyl chloride (*top*) and bromopropionyl chloride (*bottom*) at 248 nm. C-Br fission from the $n_O\pi^*_{C=O}$ excitation is identified by comparing it to kinetic energies imparted in C-Br fission in a molecule in which the repulsive electronic transition does not overlap the $n_O\pi^*_{C=O}$ transition to the $^1A''$ potential energy surface of interest. Note that the $P(E_T)$ for bromopropionyl chloride, shown in *solid circles* in the bottom frame, corresponds almost exactly to a $P(E_T)$ characteristic of dissociation upon excitation of the overlapping $n_{p,Br}\sigma^*_{C\text{-}Br}$ transition (*squares*) with minimal or no contribution from the overlapping $n_O\pi^*_{C=O}$ transition. (Adapted with permission from Figures 7 and 8 of Reference 57, copyright 1993, American Institute of Physics.)

both systems, about 200 cm^{-1} in bromoacetyl chloride and about 20 cm^{-1} in bromopropionyl chloride at typical $R_{C=O}$ geometries near 1.2 Å, is so small that a simple Landau-Zener calculation shows that fewer than five percent of the reactive events that would lead to C-Br bond fission on the adiabatic potential surface actually cross the barrier adiabatically.[6] The other 95% (or more in bromopropionyl chloride) retain the $n_O\pi^*_{C=O}$ configuration at the avoided crossing and hop to the upper adiabat, resulting in the trajectories turning back toward the reactant region. In bromopropionyl chloride, the energetic splitting is a factor of ten smaller than in bromoacetyl chloride, on the order of 20 cm^{-1}, so one expects the nonadiabatic recrossing to increase by a factor of one hundred, consistent with the experimentally observed suppression of C-Br fission upon $^1(n_O\pi^*_{C=O})$ excitation. Thus the calculations and experiments on bromopropionyl chloride, designed to test the intramolecular distance dependence of the splitting and the resulting nonadiabatic recrossing of the barrier to C-Br fission, confirm that the additional intervening bond further suppresses C-Br fission by at least an order of magnitude.

CLASSES OF CHEMICAL REACTIONS SUBJECT TO FAILURE OF THE BORN-OPPENHEIMER APPROXIMATION

The experiments above encourage us to identify what classes of chemical reactions are subject to such a dramatic reduction in their rate owing to nonadiabatic recrossing of the reaction barrier. Reactions that traverse a conical intersection along the reaction coordinate have long been understood to be susceptible to nonadiabatic effects. The last subsection here describes how such nonadiabatic effects slow the rate of reactions normally referred to as "(overall) symmetry forbidden," since those reactions are ones that traverse a conical intersection, and the last section of the review article includes examples of how nonadiabatic recrossing can be mediated by the location at which the reactive trajectories traverse a conical intersection. This section begins, however, by reviewing the work that identified reactions known as "Woodward-Hoffmann-forbidden" as a second class of reactions also particularly susceptible to nonadiabatic effects. I begin in the next subsection by outlining why this class of reactions can have anomalously small energetic splittings between adiabats at the reaction barrier and thus can evidence a substantial reduction in rate as a result of nonadiabatic recrossing. The later subsections review the first few series of experiments that developed the premise that these reactions are anomalously slow because of nonadiabatic recrossing. Molecular conformation plays a key role in several

[6]The details of this back-of-the-envelope estimate are given in Reference 56 (56:1584).

of the experiments, because with a conformation change, a reaction path in the same molecule can change from formally Woodward-Hoffmann forbidden to formally Woodward-Hoffmann allowed.

Identifying Woodward-Hoffmann Forbidden Reactions as a Class Subject to Nonadiabatic Recrossing: Background and Theory

In the class of reactions designated as Woodward-Hoffmann (W-H) forbidden, individual electronic orbital symmetry is not conserved along the reaction coordinate (46, 58a), and the barrier resulting from the avoided crossing is often cited as the reason why these reactions are unfavorable.[7] The text by Woodward and Hoffmann states "To put the matter in other words, there is a very large symmetry-imposed barrier to the reactions..." and adds in the next paragraph that although the crossing is avoided "...the reaction still must pay the price in activation energy for the intended but avoided crossing" (58a). They clearly imply that the dynamics proceeds on the lower adiabat, with the only price being the energetic barrier to the reaction. However, the experiments and calculations, detailed in the section above on the Woodward-Hoffmann forbidden excited state C-Br bond fission reaction, showed that the reaction was not disfavored because of a higher energy barrier compared to the competing reaction pathway; rather it was "forbidden" because of a very high nonadiabatic recrossing probability. The nuclear dynamics nonadiabatically hops to the upper $2^1A''$ adiabat as it tries to cross the transition state, and thus unexpectedly turns back from the avoided crossing region at energies well above the barrier, markedly reducing the reaction rate constant. I argue below that this class of reactions, ones where the individual orbital symmetry changes along the adiabatic reaction path, should show anomalously small splittings at the avoided crossing that forms the reaction barrier. Hence, nonadiabatic recrossing of the reaction barrier may be the dominant reason why Woodward-Hoffmann forbidden reactions are unfavorable even when there is sufficient energy to surmount the barrier to the reaction.

To qualitatively argue why this class of reactions should show anomalously small splittings at the reaction barriers, I consider a comparison between reactions that have a barrier formed from an avoided crossing between electronic configurations where both individual orbital symmetries and overall electronic state symmetry are conserved, versus ones where overall symmetry is conserved but individual orbital symmetry is not. The argument closely follows that of

[7]This section refers to the *general* definition of Woodward-Hoffmann forbidden reactions, not limiting them to pericyclic reactions (a common subclass). The importance of narrowly avoided curve crossings as a route to internal conversion in photochemical rearrangements was detailed in early work by Carr et al (58b) and Yang et al (58c).

Silver (47), who put forward the idea of differences in the "barrier energy lowering" from the diabatic crossing for these two classes of reactions. Although I retain much of his argument (the splitting between adiabats is twice the "barrier energy lowering"), I emphasize that the critical point here is that the height of the barrier, on which Silver focused, is not as important for these systems as the probability of crossing the barrier adiabatically.

Using the Woodward-Hoffmann forbidden reaction described in the section above as an example, consider the dominant electronic configuration contributing to the electronic wavefunction, Ψ_R, on the reactant side of the barrier, represented by one electron in an n_O orbital and another in a $\pi^*_{C=O}$ orbital, and the dominant configuration contributing to the electronic wavefunction, Ψ_P, on the product side of the barrier, represented by one electron in an n_x orbital and one in a $\sigma^*_{C\text{-}X}$ orbital (where X = Cl or Br). The reactant configuration, $\{\ldots(n_X)^2(n_O)^1(\pi^*_{C=O})^1(\sigma^*_{C\text{-}X})^0\}$, differs from that on the product side of the barrier, $\{\ldots(n_X)^1(n_O)^2(\pi^*_{C=O})^0(\sigma^*_{C\text{-}X})^1\}$, by two electrons. Configuration interaction matrix elements mix and split these two electronic configurations at the avoided crossing that forms the barrier to C-X bond fission. In this two-state model, with no orthogonality assumed between reactant and product molecular orbitals or between Ψ_R and Ψ_P, the general expression for the splitting between the adiabatic Born-Oppenheimer potential energy surfaces is:

$$\text{Splitting} = 2(\beta - \alpha S)(1 - S^2)^{-1}, \qquad 3.$$

in which α = the energy at which the diabats cross, S = the overlap integral $\langle\Psi_R|\Psi_P\rangle/C$, β = the interaction, resonance, or exchange energy $\langle\Psi_R|H|\Psi_P\rangle/C$, and C corrects for unnormalized wavefunctions.[8]

However, for Woodward-Hoffmann forbidden reactions, such as C-Cl and C-Br bond fission on the lowest $^1A''$ electronic state of bromoacetyl and bromopropionyl chloride, the overlap integral S is zero because individual orbital symmetry is not conserved. In planar C_S conformers of bromoacetyl- and bromopropionyl chloride, the $\pi^*_{C=O}$ orbital has a$''$ symmetry while the $\sigma^*_{C\text{-}X}$ orbital has a$'$ symmetry so the overlap integral $\langle\pi^*_{C=O}|\sigma^*_{C\text{-}X}\rangle = \langle a''|a'\rangle = 0$. Similarly, the n_X orbital has a$''$ symmetry while the n_O orbital has a$'$ symmetry, so the overlap integral $\langle n_X|n_O\rangle = \langle a''|a'\rangle = 0$. Because individual orbital symmetry is not conserved for Woodward-Hoffmann forbidden reactions, all one-electron integrals that contribute to the resonance and exchange energy represented by β above are also zero, leaving only two-electron integrals to mix and split the

[8]This splitting is twice the energy lowering ΔE on which Silver (47) focused, but in that article the expression given in Equation 15 for the energy lowering ΔE from the diabatic crossing energy is incorrect. The correct expression for $2\Delta E = 2V_{12}$, given above in Equation 3, is also given in Reference 14, footnote 20, and may be easily derived from Equation 9 in Silver's article.

electronic states at the avoided crossing (47).

$$2V_{12} = \text{splitting in W-H forbidden reactions} = 2\beta_2 \qquad 4.$$

Thus the splitting between the adiabats at the barrier is expected to be anomalously small for this class of reactions. Indeed, our simple electronic structure calculations on the Woodward-Hoffmann forbidden reactions in $Br(CH_2)_nCOCl$, described above and in (57), showed the splitting is on the order of hundreds of wavenumbers for both C-Br and C-Cl fission in bromoacetyl chloride and on the order of only tens of wavenumbers for C-Br fission in bromopropionyl chloride. In addition, there is preliminary computational evidence that upon breaking the symmetry element that makes the reaction Woodward-Hoffmann forbidden, as in the *gauche* conformers of bromoacetone and allyl chloride discussed in the next subsections, the splitting increases considerably.

These results show that the commonly held notion that Woodward-Hoffmann forbidden reactions are unfavorable because of their large barrier misses a key point: In bromopropionyl chloride, the Woodward-Hoffmann forbidden C-Br fission was forbidden not because the barrier was too high (indeed the C-Cl fission channel with a 10 kcal/mole higher barrier was the dominant product!), it was suppressed instead by the electronic nonadiabaticity as reactive trajectories try to cross the transition state, because of the anomalously small splitting between adiabats at the reaction barrier.

Conformational Dependence of Nonadiabatic Recrossing: Background and Computational Results on Bromoacetone

The experiments detailed above investigated one of the simplest but most chemically important consequences of the failure of the Born-Oppenheimer approximation: the marked change in the expected branching between energetically allowed chemical bond fission channels that result from nonadiabatic recrossing of a reaction barrier. I proposed that in Woodward-Hoffmann forbidden reactions, the nonadiabatic recrossing is particularly severe because the reversal of individual orbital symmetries along the reaction coordinate results in an anomalously small energetic splitting between adiabats at the transition state and thus a high nonadiabatic recrossing probability. One important way to test this hypothesis is to examine the conformation dependence of a photodissociation reaction where the reaction is Woodward-Hoffmann forbidden in planar geometry, but formally Woodward-Hoffmann allowed in the nonplanar conformer. It can be anticipated that the rate of the chemical reaction, or its branching ratio with respect to other product channels, will be significantly enhanced for the nonplanar conformer.

Molecular conformation thus affords the opportunity to test whether a reaction channel that is Woodward-Hoffmann forbidden has a smaller splitting

between adiabats at the reaction channel—and thus is more susceptible to nonadiabatic recrossing—than a reaction that is not Woodward-Hoffmann forbidden. Early computational results (59, Table 1) on the C-Br fission reaction channel in $n_O\pi^*_{C=O}$ excited bromoacetone demonstrate the point. In the planar conformer, misnamed the *trans* conformer[9] by early spectroscopists in analogy with XCH_2COCH_2X, C-Br fission, is formally Woodward-Hoffmann forbidden because the n_{Br} and $\sigma^*_{C\text{-}Br}$ orbitals of the product electronic configuration on the $^1A''$ adiabat have the reversed symmetry, a'' and a' respectively, compared to the $a'n_O$ and $a''\pi^*_{CO}$ orbitals in the reactant electronic configuration. As expected from the argument given in the preceding section, simple ab initio electronic structure calculations indicate that the avoided crossing between these two configurations that form the reaction barrier on the A'' potential energy surface is only narrowly avoided and thus susceptible to nonadiabatic recrossing. One can easily make the same reaction channel formally Woodward-Hoffmann allowed by considering C-Br fission from the nonplanar conformer (again, misnamed the *gauche* conformer). The calculated potential energy surfaces for this nonplanar conformer given in (59, Table 1) show a significant increase in the energetic splitting at the avoided crossing over that calculated for the planar conformer; relevant cuts through the avoided crossing are shown in Figure 7 for both conformers. Thus, C-Br fission can proceed much more adiabatically in the gauche conformer, where the reaction is formally Woodward-Hoffmann allowed than in the planar conformer.

In a standard CIS calculation one begins with an orthogonal basis, so in both conformers only two-electron integrals contribute to the off-diagonal matrix elements. Even so, this recovers the result derived in the section above, assuming no orthogonality, that the Woodward-Hoffmann forbidden reaction shows a smaller splitting at the avoided crossing than the Woodward-Hoffmann allowed reaction. This is simply because the influence of the larger overlap densities in the gauche conformer results in an orthogonal basis where there are no longer local $\sigma^*_{C\text{-}Br}$ and $\pi^*_{C=O}$ orbitals; the orthogonal orbital basis shows an admixture with the n_O and np_{Br} orbitals respectively and thus the electron configuration interaction matrix elements are larger (giving a larger splitting despite only two-electron integrals being nonzero at the CI level). In bromoacetone it was not possible to test this prediction experimentally, since C-Br fission occurs in competition with a second reaction channel, C-C fission, which is even more strongly influenced by molecular conformation. Indeed the measured (59, 60)

[9]The planar bromoacetone and chloroacetone conformers that I refer to here as *trans* or *anti* should, in correct nomenclature, be called *s-cis*, because the dihedral angle between the C-Cl(Br) and the C=O bond is zero and the halogen and O atoms, having the highest atomic numbers, should determine the groups to which the geometry refers. However, I retain the nonstandard name of *trans* for this conformer in order to remain consistent with several earlier studies.

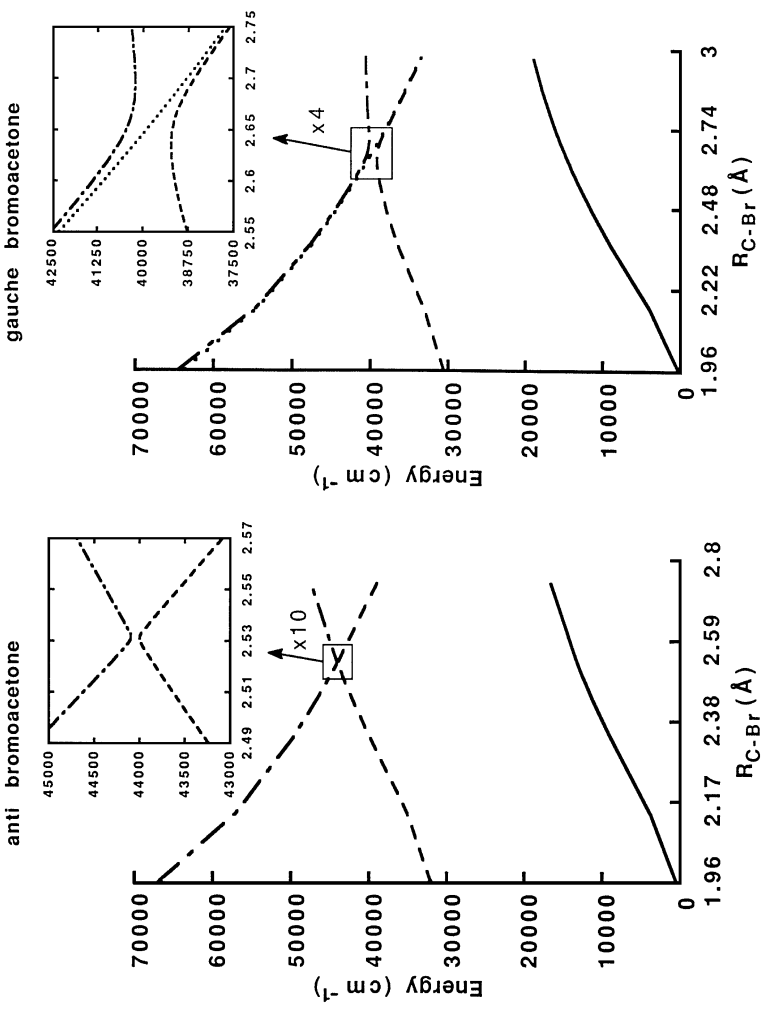

Figure 7 Cuts through the calculated ab initio potential energy surfaces for *gauche* bromoacetone (*right*) with $r_{C=O} = 1.280$ Å and *anti* bromoacetone (*left*) with $r_{C=O} = 1.282$ Å (see footnote in text for nonstandard naming of conformers). Although for the *gauche* conformer all three electronic configurations can mix and split, it appears that one does not interact strongly with the other two. The insets show that the splitting between the adiabats at the barrier to C-Br fission in *anti* bromoacetone is smaller by at least a factor of eight than that in *gauche* bromoacetone. Other cuts are given in Table 1 of Reference 59. (Reproduced with permission from Figure 12 of Reference 59, copyright 1994, American Institute of Physics.)

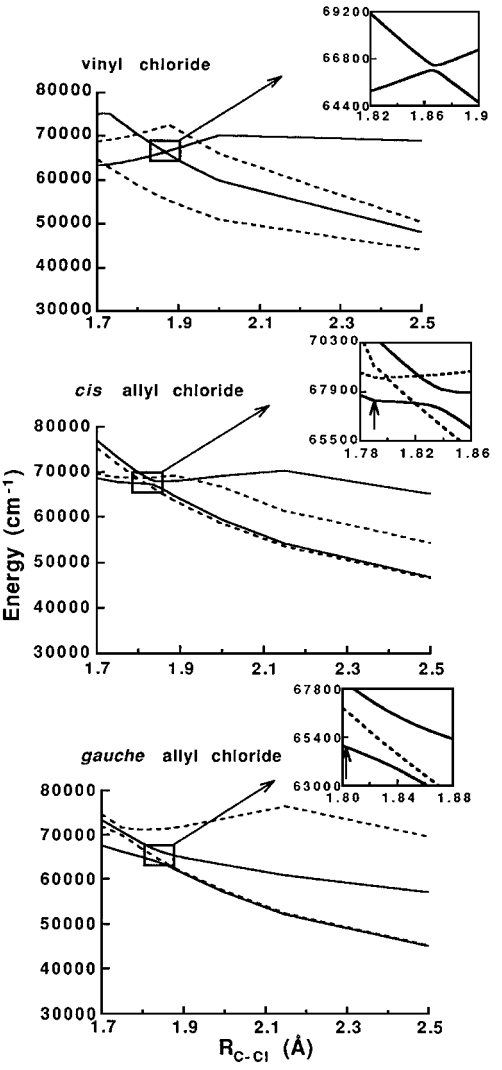
vinyl chloride
69200
66800
64400
1.82
1.86
1.9
80000
70000
60000
50000
40000
30000
1.7
1.9
2.1
2.3
2.5
cis allyl chloride
70300
67900
65500
1.78
1.82
1.86
Energy (cm-1)
gauche allyl chloride
67800
65400
63000
1.80
1.84
1.88
RC-Cl (Å)

absolute C-Br:C-C fission branching ratio $= k_{C\text{-}Br}/k_{C\text{-}C}$ and increases upon thermal excitation to the higher energy planar conformer, from 1.4 at 100°C to 2.3 at 400°C, rather than decreasing as would have been expected based on the C-Br channel alone. Plainly, the rate constant for C-C fission is much lower in the planar conformer. However, the systems of vinyl and allyl chloride can be used to test whether a molecular conformation that renders a reaction as Woodward-Hoffmann allowed significantly decreases the nonadiabatic suppression of the rate. Those results are reviewed in the next subsection.

Conformational Dependence of Nonadiabatic Recrossing: C-Cl Fission in Gauche Allyl Chloride

The experiments and supporting ab initio calculations on the competing photodissociation pathways for allyl chloride upon excitation of the nominally $\pi\pi^*_{C=C}$ transition at 193 nm further explored how configuration interaction matrix elements can change with molecular conformation, influencing both nonadiabatic recrossing and product branching (61, 62). The C-Cl fission reaction channel is formally Woodward-Hoffmann forbidden both in vinyl chloride and in the minor conformer of allyl chloride, which has a plane of symmetry, but not in *gauche* allyl chloride.[10] Thus, a measurement of the conformation

[10]The switch in individual orbital symmetry characterizes the reaction coordinate if it is from a $\pi\pi^*_{C=C}/n_{Cl}\sigma^*_{C\text{-}Cl}$ avoided crossing, but Reference 63 indicates the reaction may proceed via a conical intersection with the $\pi_{C=C}\sigma^*_{C\text{-}Cl}$ state in vinyl chloride, so it may also in allyl chloride.

←

Figure 8 Cuts through the calculated ab initio electronic surfaces at equilibrium C=C bond lengths, for vinyl chloride (*top*), *cis*-allyl chloride (*middle*), and *gauche*-allyl chloride (*bottom*). In the top and middle frames, the four lowest singlet excited electronic states are shown. The two A′ adiabatic states (*solid lines*) are involved in the avoided electronic configuration crossing. The two A″ adiabatic states (*dashed lines*) do not interact with the A′ states. For the particular cut along the avoided crossing seam presented here, the splitting at the avoided crossing to C-Cl bond fission enlarged in the insets is 261 cm^{-1} for vinyl chloride and 982 cm^{-1} for *cis*- allyl chloride. In the *gauche* conformer, only the three lowest singlet excited electronic states are shown (the next singlet excited state is above 70,000 cm^{-1}). Because the symmetry is broken, the BB* character can, in principle, mix into all three electronic states so that a two-state approximation may no longer be valid. By tracking the oscillator strengths (predominantly from BB* character) and the dominant electronic configurations of the excited state potential energy surfaces along the $R_{C\text{-}Cl}$ coordinate, one can determine that primarily the first and third excited states (*solid lines*) exhibit an avoided crossing around 1.84 Å. (The second excited state surface (*dashed*) does not participate significantly until 1.86 Å.) For the particular cut along the avoided crossing seam presented here, the splitting at the avoided crossing between the first and third adiabats is 2626 cm^{-1}. For the *cis* and *gauche* conformers of allyl chloride, the insets also includes the Franck-Condon region (*arrow*). (Adapted with permission from Figures 13 and 14 of Reference 61, copyright 1996, American Institute of Physics.)

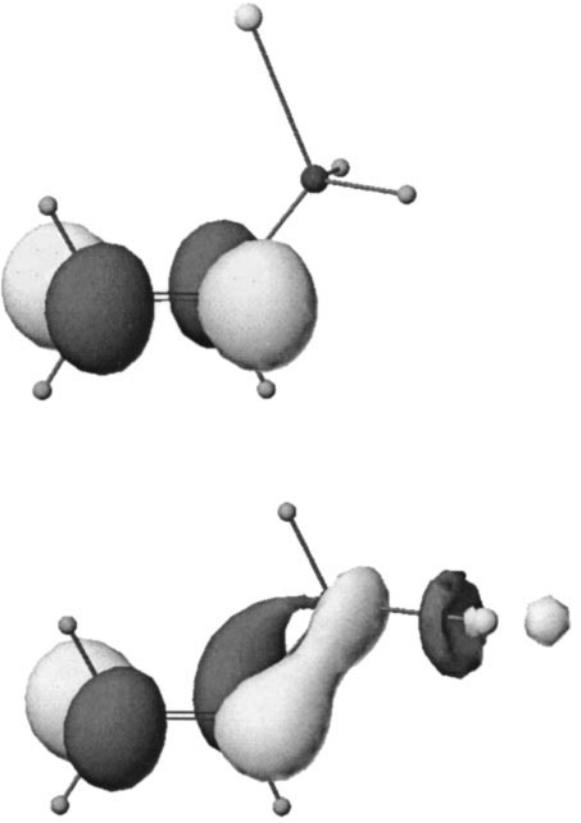

Figure 9 The top frame shows the excited state molecular orbital for *cis* allyl chloride from the bright state in the Franck-Condon region. The orbital illustrates the essentially pure $\pi^*_{C=C}$ character. The bottom frame shows the dominant excited state molecular orbital for *gauche*-allyl chloride from the bright state in the Franck-Condon region. The orbital has an admixture of $\pi^*_{C=C}$ and $\sigma^*_{C\text{-}Cl}$ character. (Reproduced with permission from Figure 6 of Reference 62, copyright 1996, American Institute of Physics.)

dependence of the C-Cl fission:HCl elimination branching ratio can determine if there is evidence for increased C-Cl fission in *gauche* allyl chloride. The measured photofragment velocity distributions evidence C-Cl bond fission and two primary processes for HCl elimination, complicating the analysis, but the results clearly showed that the branching to C-Cl fission is higher than in vinyl chloride, where C-Cl fission in the excited state is Woodward-Hoffmann forbidden, and that molecular conformation influences the branching ratio. The experimental measurements show that C-Cl bond fission dominates, giving an absolute

branching ratio of HCl:C-Cl $= 0.30 \pm 0.03$:1 when the parent molecule is expanded through a nozzle at 200°C and HCl:C-Cl $= 0.59 \pm 0.06$:1 when the population in the *cis* conformer is increased by heating the nozzle to 475°C (63).

Analysis of the experimental results (61, 62, 64; Y-R Lee & S-M Lin, submitted for publication) along with supporting ab initio calculations on both conformers of allyl chloride and on vinyl chloride (65–67a) reveals two things. Figure 8 shows cuts along the excited state C-Cl fission reaction coordinate in vinyl chloride (*top*), *cis* allyl chloride (*middle*), and *gauche* allyl chloride (*bottom*). The figure shows that the avoided electronic curve crossing [$\pi\pi^*_{C=C}(a''a'')$ to $n\sigma^*_{C\text{-}Cl}(a'a')$], which forms the barrier to C-Cl fission on the excited state surface, is very narrowly avoided in both vinyl and *cis* allyl chloride, which have a plane of symmetry, but not in *gauche* allyl chloride. This work thus helps demonstrate the generality of the conclusion that Woodward-Hoffmann forbidden reactions are subject to a reduction in rate constant from nonadiabatic recrossing. One can also see the effect of the stronger off-diagonal matrix elements between the $\pi\pi^*_{C=C}$ to $n\sigma^*_{C\text{-}Cl}$ electronic configurations in the *gauche* conformer when one looks at the shape of the excited state potential energy surface in the Franck-Condon region. The excited state potential energy surface in *gauche* allyl chloride shown in Figure 8 (*bottom*), is already somewhat repulsive in the C-Cl reaction coordinate even in the Franck Condon region. (This doubtless also influences the product branching). This indicates that even before the avoided crossing, the large configuration interaction matrix elements in *gauche* allyl chloride result in an admixture of the $n\sigma^*_{C\text{-}Cl}$ configuration into the nominal $\pi\pi^*_{C=C}$ excited state. The partial $\sigma^*_{C\text{-}Cl}$ character is easily seen in Figure 9, which compares the "nominal" $\pi^*_{C=C}$ orbital reached at the equilibrium geometry of the ground state for *cis* allyl chloride and *gauche* allyl chloride; this admixture in the Franck-Condon region also reveals itself in the emission from the dissociating molecules, which shows intensity in the C-Cl stretch in allyl chloride but not in vinyl chloride (62). An analogous conformation dependence to the $\pi^*_{C=O}\sigma^*_{C\text{-}Cl}$ mixing is observed in the β-chloroketones (67b).

Conformational Dependence of Nonadiabatic Recrossing and Its Influence on Organic Photoreactivity

Some of the more beautiful examples of the influence of the conformational dependence of nonadiabatic recrossing on organic photoreactivity are represented in the work on the *exo*, *endo*, *anti*, and *syn* isomers of chlorine-substituted norbornenes by Morrison, Jordan, and co-workers (68, 69). C-Cl bond fission can result from an avoided electronic configuration crossing between an initially excited $\pi\pi^*$ excited configuration and an $n\sigma^*_{C\text{-}Cl}$ dissociative configuration. The photolysis experiments on the isomers of 7-chlorobenzonorbornene show that the exo and anti conformers show greatly enhanced reactivity as a result of

primary C-Cl bond photoreactivity. Complementary natural bond orbital electronic structure calculations show that the *anti* and *exo* structures allow a strong mixing between the σ^* and π^* orbitals, much like that in gauche acetyl chloride described in the previous subsection. This allows for efficient adiabatic traversal of the avoided crossing, while the endo and syn conformers evidence nearly no mixing in the calculation and show greatly reduced (by a factor of 30 or more) photoreactivity because of nonadiabatic recrossing. Much of the organic literature describes the chemistry in an approximately diabatic representation, where strong off-diagonal potential coupling (often termed "through space" and "through bond" coupling to connect with studies of intramolecular electronic energy transfer) promotes the transition from the $\pi\pi^*$ excited configuration to the $n\sigma^*_{C\text{-}Cl}$ configuration at the avoided crossing (the adiabatic traversal of the avoided crossing).

Electronically Nonadiabatic N-OH Bond Fission in $1^1A'$ Nitric Acid

So far I have shown that reactions in which the individual orbital symmetries change along the adiabatic reaction path are particularly susceptible to electronically nonadiabatic effects. The 193-nm photodissociation of nitric acid (71a) reviewed in this subsection shows that not only can the rate of such individual orbital symmetry-forbidden reactions be diminished substantially by nonadiabatic recrossing, but that one can also observe a second reaction channel that would not have been accessed if the reaction dynamics were adiabatic. Furthermore, the work suggests a hierarchy, represented in a back-of-the-envelope "restricted" correlation diagram, in what reaction paths are electronically possible or impossible. (See 71b for a recent review of further results.) Reaction channels that reverse the individual orbital symmetries are hard enough, but ones that require orbital symmetries to change on two electronically isolated functional groups are virtually impossible. The potential significance to chemical reactions in gas or condensed phase molecules with spatially separated functional groups is clear (71a,b).

Although it had long been known that both formation of OH + NO_2 and formation of O + HONO occurred in the 193-nm photodissociation of nitric acid (72–74; CE Miller, HF Davis, YT Lee, private communication and unpublished results; 75–77), recent work (71a) shows that both processes exhibit two competing mechanisms, one adiabatic channel and one nonadiabatic. A photofragment time-of-flight spectrum showing the competing channels is depicted in Figure 10. I now focus on the two competing mechanisms, previously misassigned (73, 78), for fission of the N-OH bond to form OH + NO_2. The $\pi_{nb,O} \rightarrow \pi^*_{NO_2}$ excitation at 193 nm accesses the $2^1A'$ excited state potential energy surface of nitric acid, which has local B_2 electronic symmetry at the nitro

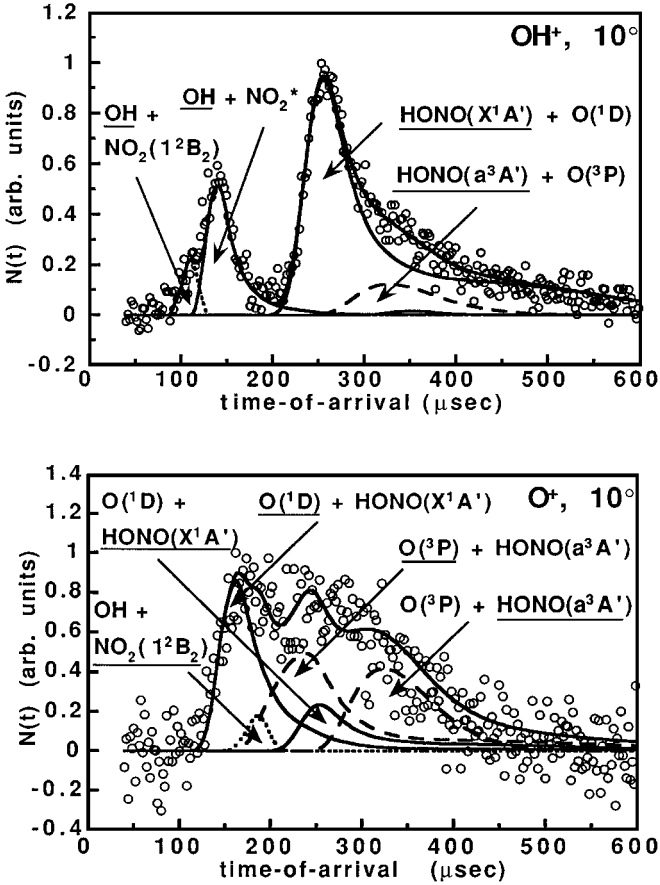

Figure 10 Laboratory time-of-flight spectra of the photofragments of nitric acid at 193 nm detected at OH^+ (*top*) and at O^+ (*bottom*). The fast peaks in the top spectrum result from two OH + NO_2 channels, one the adiabatic asymptotic products and one nonadiabatic. The slow signal results from two O + HONO channels. *Solid lines* and *dashed lines* show the forward convolution fits to each of the product channels obtained with the $P(E_T)$'s given in Reference 71a. (Adapted with permission from Figures 1 and 5 of Reference 71a, copyright 1997, American Institute of Physics.)

group (79, 80). This Born-Oppenheimer potential energy surface correlates adiabatically to OH + $NO_2(1^2B_2)$ at bent NO_2 geometries, but this low-lying doublet B_2 electronic state of NO_2 does not have the same $\pi_{nb,O}\pi^*_{NO_2}$ character as the NO_2 group in nitric acid had in the Franck-Condon region. Thus, along the N-OH fission reaction coordinate, the electronic configuration at the NO_2 group must change from $\pi_{nb,O}\pi^*_{NO_2}$ in character to the dominant electronic configuration of the $NO_2(1^2B_2)$ asymptotic fragment, $\{\ldots(4b_2)^1(6a_1)^1\}$. This is exactly the kind of electronic change along an adiabatic reaction coordinate that makes the reaction subject to nonadiabatic effects; the individual NO_2 orbital symmetries change from a″a″ in the reactant region to a′a′ in the product region along the $2^1A'$ excited-state potential energy surface (the adiabatic reaction products are Woodward-Hoffmann forbidden). Thus, one expects the reaction path to be difficult to follow owing to the electronic changes required, and indeed one sees that another N-OH fission reaction channel is thus able to compete effectively with it (the one with OH arrival times near 130 ms in Figure 10).

The experiments reviewed above developed and tested the premise that for the class of reactions in which the overall symmetry is conserved along the reaction coordinate, but individual orbital symmetry is not, the probability of adiabatically crossing this barrier for trajectories with enough energy to do so is dramatically reduced by nonadiabatic effects. I now consider another class of reactions more commonly understood to be subject to nonadiabatic effects.

"Overall Symmetry-Forbidden" Chemical Reactions and the Breakdown of the Born-Oppenheimer Approximation Near a Conical Intersection

Although it has long been understood that the Born-Oppenheimer approximation can break down near a conical intersection, the importance of this phenomenon in organic reactions described as overall "symmetry-forbidden" is less well understood by the general community. The physical organic literature describes some classes of reactions, such as a Norrish Type-I C-C fission, as "overall symmetry-forbidden" because the reactant electronic configuration has, for instance, A″ electronic symmetry and the product electronic configuration has A′ symmetry. This section addresses the underlying physical reason that explains why these reactions have slow rates. First, the reader should note that the common terminology "symmetry-forbidden" is misleading because the reaction is formally only forbidden by *symmetry* at a singularity on the potential energy surface; at any geometry that deviates at all from planarity, the reaction is actually perfectly symmetry-allowed on the adiabatic potential energy surface. I thus argue below that the true physical basis for the slow rate

of reactions commonly termed "symmetry-forbidden" is actually the breakdown of the Born-Oppenheimer approximation as nuclear trajectories attempt to traverse the transition state *near* the conical intersection. This model, presented below, was originally proposed (59) to rationalize the conformation dependence of the C-C fission channel in bromoacetone, but it is likely that this particular system is much more complicated (60) than originally thought. Thus, although I present the model in the context of bromoacetone below, the reader should note that it is too simple a description for that system. Rather, the importance of the model below lies in its description of the way in which the Born-Oppenheimer breakdown provides the physical basis for the "forbiddenness" of reactions that, although commonly termed "symmetry forbidden," are only formally forbidden by symmetry at a singularity on the potential energy surface.

Consider an "overall symmetry-forbidden" unimolecular reaction where the dynamics is initiated (perhaps by absorption of a photon or by thermal excitation in the case of ground state reaction) on a potential energy surface that has A'' symmetry. The $n_O\pi^*_{C=O}$ excited state of bromoacetone provides an illustrative example. Experimentally, one observes a competition between C-Br fission and C-C fission, and photofragment anisotropy measurements (59) establish that the branching ratio favors C-Br fission from the planar anti-conformer and C-C fission from the gauche (nonplanar) conformer (see footnote above on the misnaming of the conformers). The electronic state leading to C-C fission has $\sigma\sigma^*_{C\text{-}C}$ character in the exit channel, a configuration with A' symmetry in $n_O\pi^*_{C=O}$ planar geometries, so in order to dissociate, the molecule must cross from an A'' potential energy surface to an A' potential energy surface.[11] Thus, the C-C fission channel would be designated "symmetry-forbidden." Indeed, in planar geometries, the electronic configuration interaction matrix elements between these two configurations are zero by symmetry, and the crossing between the A'' surface and the A' surface is not avoided; the A'' potential energy surface in the Franck-Condon region does not correlate adiabatically to ground state C-C fission products. The upper adiabat and the lower adiabat depicted in Figure 11 thus touch at planar geometries along the C-C fission reaction coordinate.

However, even zero point motion in the torsional angle α depicted in Figure 11 breaks the plane of symmetry, and this allows the $n_O\pi^*_{C=O}$ and the $\sigma_{C\text{-}C}\sigma^*_{C\text{-}C}$ electronic configurations to mix and split at the crossing. A conical intersection

[11]The repulsive electronic configuration leading to C-C fission with $\sigma\sigma^*_{C\text{-}C}$character in the exit channel would be a triplet, but for the sake of simplicity, I neglect any consideration of spin symmetry. While this may be a tolerable omission in the case of bromoacetone, it is certainly not acceptable for the real system in chloroacetone. Thus this discussion should be considered a hypothetical one for the case of pedagogy. The real C-C fission dynamics in $n_O\pi^*_{C=O}$excited chloroacetone and bromoacetone are certainly more complicated.

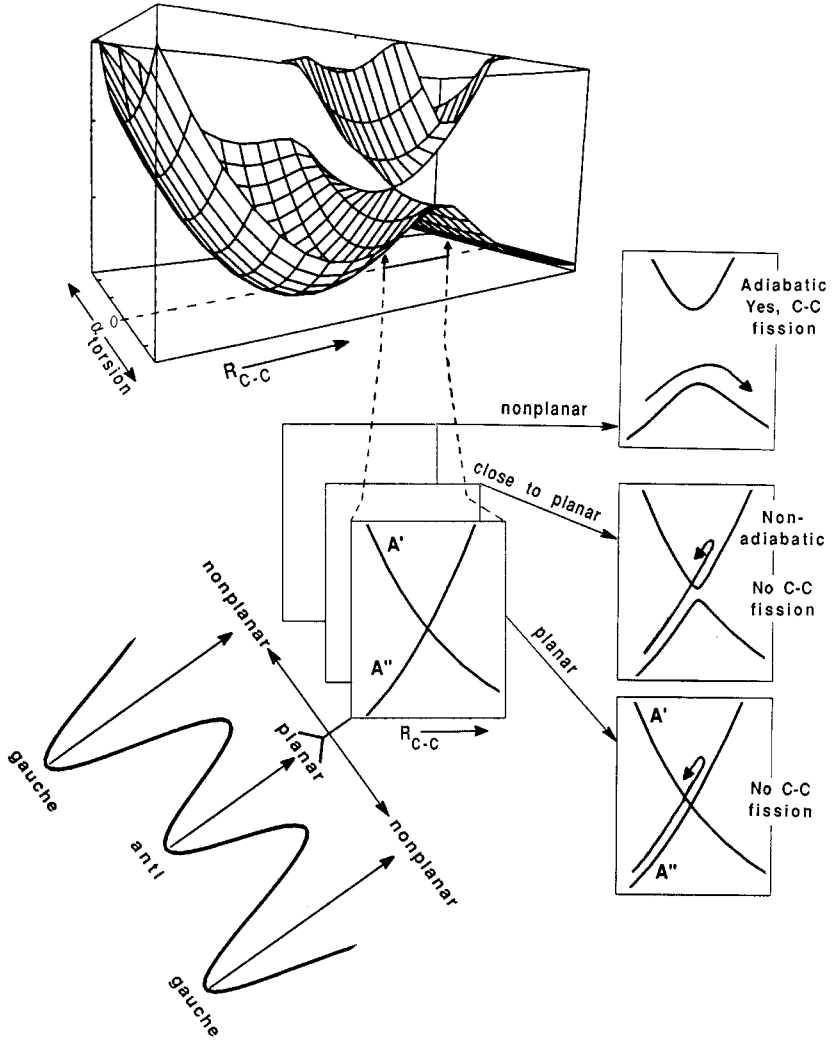

Figure 11 Schematic representation of the different regions of the conical intersection along the C-C fission reaction coordinate sampled by dissociating the *anti* versus the *gauche* conformer. The frames on the *right side* of the figure show three slices through the conical intersection: at planar geometry ($\alpha_{\text{torsion}} = 0$) (*bottom*); at close to planar geometries (small α) where the adiabats are weakly split, so nonadiabatic recrossing dominates the dynamics (*middle*); and at highly nonplanar geometries, sampled by dissociative trajectories from the *gauche* conformer, where the adiabats are strongly split so C-C fission can proceed adiabatically (*top*). (Adapted with permission from Figure 13 of Reference 59, copyright 1994, American Institute of Physics.)

along the C-C fission reaction coordinate results, as depicted schematically in the figure. Clearly, nuclear dynamics initiated on the lower adiabatic potential energy surface can evolve adiabatically to ground state products as long as they do not cross the transition state right at the point of conical intersection. Thus, the reaction is not "symmetry-forbidden" except for an infinitesimally small number of the reactive trajectories. However, the splitting between the upper and lower adiabats near the conical intersection is quite small, so it is unlikely that reactive trajectories that attempt to cross the transition state in close to planar geometries will do so adiabatically; instead, they will retain bound $n_O \pi^*_{C=O}$ electronic character, thus undergoing a hop to the upper bound adiabat, and reverse direction to return to the Franck-Condon region rather than dissociating at the C-C bond. It is these geometries that are accessed when one photodissociates the *anti* conformer, so nonadiabatic recrossing of the C-C fission reaction barrier near the conical intersection results in C-C fission being unable to compete effectively with C-Br fission in the *anti* conformer, as depicted schematically in Figure 11. Conversely, photodissociation of the *gauche* conformer allows Franck-Condon access to dissociative wavefunctions that traverse the conical intersection at nonplanar geometries where the adiabats avoid each other strongly, so C-C fission can proceed adiabatically. The lack of observation of C-Br fission from the *gauche* conformer would suggest in this oversimplified model that once C-C fission can proceed more adiabatically, it dominates C-Br fission. A final experimental measurement attempted to test this model by changing the relative population of *anti* and *gauche* conformers in a reactant molecular beam and determining how the observed branching ratio between C-C and C-Br fission changes. Figure 12 shows that upon changing the nozzle temperature from 100° to 400°C, and thus decreasing the fraction of molecules in the lower energy *gauche* conformer, the branching ratio does indeed shift toward a smaller contribution from C-C fission. Changes of the branching ratio with population in each of the conformers can thus be measured, allowing us to test whether the change is consistent with a prediction that assumes that C-C fission dominates from the gauche conformer and C-Br fission dominates from the anti (planar) conformer. Assuming no cooling of conformer populations in the expansion (81), the relative change in conformer population upon heating the nozzle from 100° to 400°C is: (59)

$$\begin{matrix} 400^\circ\mathrm{C}: \\ 100^\circ\mathrm{C}: \end{matrix} \frac{\left(\frac{anti}{gauche}\right)_{400}}{\left(\frac{anti}{gauche}\right)_{100}} = \frac{(0.34)}{(0.25)} = \text{predicted} \frac{\left(\frac{\text{C-Br}}{\text{C-C}}\right)_{400}}{\left(\frac{\text{C-Br}}{\text{C-C}}\right)_{100}} = 1.4 \qquad 5.$$

giving a predicted increase in the C-Br:C-C branching ratio of a factor of 1.4 if C-C fission dominates in the *gauche* conformer and C-Br fission dominates in

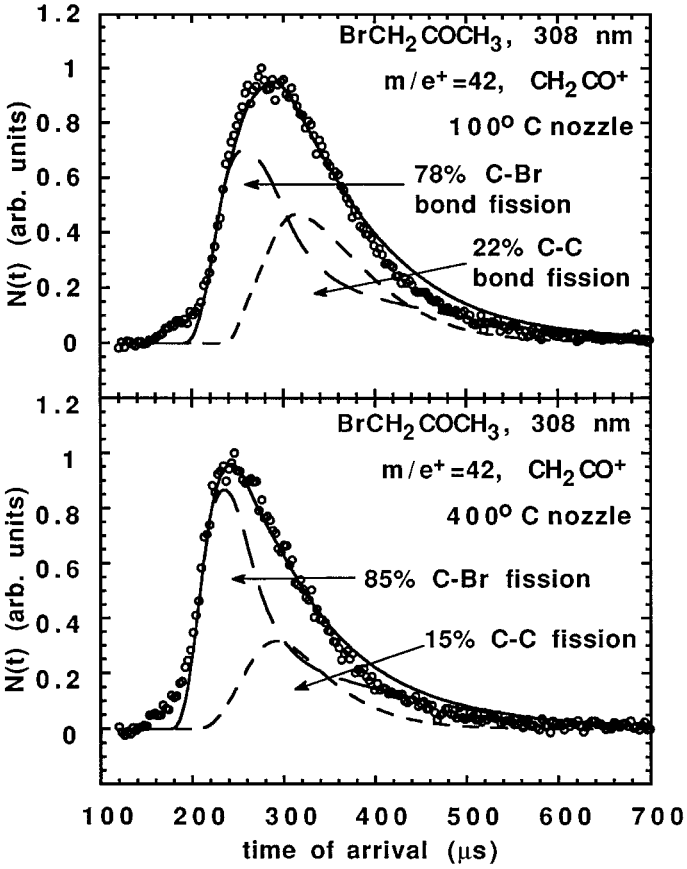

Figure 12 Laboratory time-of-flight spectra at two nozzle temperatures of the photofragments detected at CH_2CO^+ from bromoacetone photodissociated at 308 nm. *Top*, nozzle temperature of 100°C; *bottom*, nozzle temperature of 400°C. The source angle was 10° for both spectra. The percent contribution to each spectrum represents only relative contributions; the absolute C-Br:C-C bond fission branching ratio changes from 1.4:1 to 2.3:1 as one raises the nozzle temperature from 100° to 400°C (60). (Reproduced with permission from Figure 14 of Reference 59, copyright 1994, American Institute of Physics.)

the *anti* conformer.[12] The experimentally observed change in branching ratio [relative numbers are given below; absolute branching ratios estimated in (60)] is quite similar:

$$\text{observed} \frac{\left(\frac{\text{C-Br}}{\text{C-C}}\right)_{400}}{\left(\frac{\text{C-Br}}{\text{C-C}}\right)_{100}} = \frac{2.3}{1.4} = 1.6! \qquad 6.$$

The result is in accord with the model presented in which dissociation from the *anti* conformer accesses regions of the C-C fission reaction coordinate near the conical intersection, where it is nonadiabatically inhibited and so cannot compete with C-Br fission, and dissociation from the *gauche* conformer proceeds through regions of the conical intersection where the surfaces are further split from each other, so the C-C dissociation can proceed adiabatically and dominate C-Br fission. Again, the actual bromoacetone electronic structure is more complicated, but the model still proves instructive in showing that the crossing is avoided at all but planar geometries, so "electronically nonadiabatic" near (not at) the conical intersection is the more relevant descriptor for the reaction than is "symmetry-forbidden."

I have avoided using the terminology "symmetry forbidden" when describing the lack of C-C fission from the *anti* conformer because, although commonly used, this language obscures the physical reason a reaction pathway that traverses a conical intersection might be unfavorable. Indeed, the reaction is "symmetry forbidden" only through a singular point on the potential energy surface (in two degrees of freedom); even small zero point bending or torsional motion of the *anti* conformer at the transition state can put amplitude at molecular geometries where the adiabatic correlation goes smoothly from reactants to products. The reason that C-C fission in the *anti* conformer is suppressed in this simple model is that trajectories that attempt to undergo C-C fission near, but not at, the point of conical intersection sample a region of phase space where the reactant and product electronic configurations are not strongly coupled, so the configuration interaction splitting between the upper and lower adiabats is small. Instead of following the adiabatic reaction coordinate, along which the electronic wavefunction changes from $n_O \pi^*_{C=O}$ to $\sigma\sigma^*_{C\text{-}C}$ in character, the dissociative trajectory hops to the upper bound adiabat as it tries to traverse the C-C reaction barrier. Thus a reaction pathway through a conical intersection is not "symmetry-forbidden" for most dissociative trajectories; rather, it is characterized by a high nonadiabatic recrossing probability.

An interesting solution phase experimental probe of high nonadiabatic recrossing probability for a dissociation through a conical intersection is presented

[12]Conformation relaxation in supersonic expansions with He as the carrier gas is shown to be minimal (for molecules in which the barrier between conformers is greater than 400 cm^{-1}).

in the work of Wagner & Waite on photoinduced radical cleavage of triplet iodobenzophenones (82). Their measured triplet lifetimes (reflecting the dissociation rate constant through the conical intersection formed from the ^{3}n,π^* and the $^3\sigma,\sigma^*$ states) showed that the A factor for the dissociation is anomalously small. They interpret the small A factor as revealing the low transmission coefficients resulting from inefficient state interconversion, i.e. using a small 6 in a statistical expression for the reaction rate constant to correct for nonadiabatic recrossing near the conical intersection (see "Reduction in the Rate of a Chemical Reaction from Nonadiabatic Recrossing of the Reaction Barrier" above.)

Based on all experiments described above, we know how to identify the chemical reactions that are likely to exhibit a failure in the Born-Oppenheimer approximation. One need not calculate a multidimensional potential energy surface to get a rough idea of the reactions that are susceptible; one need only look at the reactant and product electronic configurations. If there is either a symmetry-imposed conical intersection near the reaction geometries accessed or a change in the individual orbital symmetries along the adiabatic reaction path, then one must be aware of potential nonadiabatic effects.

The last section of this review article describes in more detail the dynamics on multidimensional potential energy surfaces that have regions where there are conical intersections, so experimental tests of the ideas outlined in this subsection are described in that section. In particular, I show how such dynamics, and the role of nonadiabatic effects, can be sensitive to several factors in addition to molecular conformation, including the approach geometry of two reactants in a bimolecular reaction, the initial vibrational state of the reactant (in photodissociation) or reactants (in bimolecular collisions), and the collision energy or total energy. Finally, I note that conical intersections are also well understood as providing a route for internal conversion to a lower electronic state, often the ground electronic state in a photodissociation experiment. Interested readers may refer to texts by Simons (83) or by Michl & Bonačić-Koutecký (48), or to the papers of Zimmerman (84), Michl (85–87), Mielke et al (88), and to a recent review by Bernardi et al (89) for a discussion relevant to an organic photochemistry perspective.

PROBING NONADIABATIC EFFECTS AT THE TRANSITION STATE

While the experiments and calculations in the preceding and subsequent sections show the importance of electronically nonadiabatic effects as a molecule tries to traverse the barrier to a chemical reaction, it is perhaps more gratifying to access the upper and lower adiabats near the transition state of a chemical

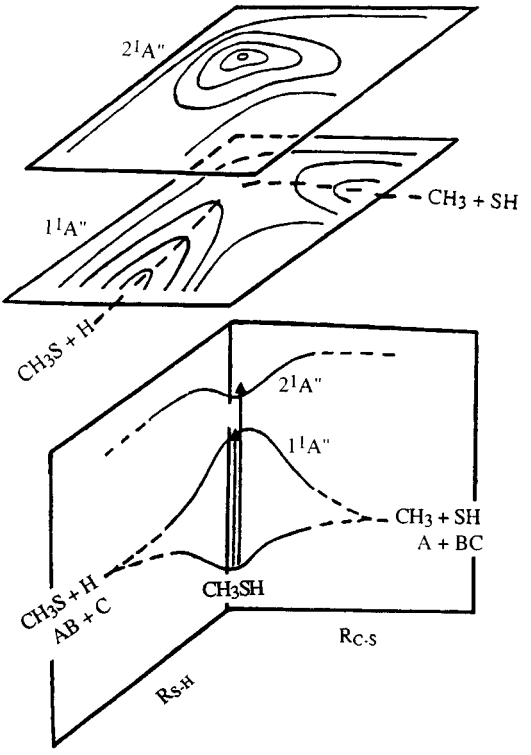

Figure 13 Schematic contour plots of the excited electronic potential energy surfaces for CH_3SH, showing the two lowest $^1A''$ adiabatic excited state surfaces. The lower diagram shows the reaction coordinate for the bimolecular reaction A + BC → AB + C along the lower excited state surface. The Franck-Condon region lies near the saddle point on the lower excited state surface. (Adapted with permission from Figure 1 of Reference 90, copyright 1993, American Institute of Physics.)

reaction more directly to probe such effects. One can do just that with the excited state reaction $CH_3S + H \rightarrow CH_3 + SH$ (90). As depicted schematically in Figure 13, excitation of CH_3SH at 222 nm offers Franck-Condon access to a region near the transition state on the lower adiabatic potential energy surface—the $1^1A''$ surface—for the excited state bimolecular reaction, since the geometry of CH_3SH in the ground electronic state is close to that of the transition state on the $1^1A''$ surface. Alternatively, when the molecule is excited at 193 nm in the higher energy absorption band, it is promoted to the upper bound adiabat—the $2^1A''$ surface—where it dissociates via nonadiabatic coupling to the transition state region of the lower adiabat. Photofragment velocity and angular distribution measurements on CH_3-S-H at 193 nm show that the

nonadiabatic decay to the transition-state region of the lower surface occurs in less than a picosecond and results in a factor of eight larger branching for decay of the transition state complex to the $CH_3 + SH$ exit channel than direct excitation to the lower adiabat at 222 nm (90–92). The larger branching ratio results from the stretching of the C-S bond on the upper adiabat, evidenced in emission spectroscopy experiments (93). These dynamics allow the molecule to sample a region of the transition state upon nonadiabatic transition to the lower dissociative surface that enhances C-S bond fission over that obtained by accessing the transition state directly via Franck-Condon excitation from the ground state. Yarkony (22, 55) has identified a conical intersection between the $1^1A''$ and $2^1A''$ surfaces that is likely responsible for the subpicosecond decay of the molecule from the upper to the lower adiabat, as evidenced by the highly anisotropic photofragment angular distributions (90, 91) upon 193-nm excitation. Early dynamics calculations (94) on the lower adiabat from the first set of potential energy surfaces (95; DR Yarkony, personal communication) for this system have begun to elucidate the dynamics, but calculations that include the nonadiabatic dynamics remain to be done. This waits, as in many other systems, for calculations of the derivative coupling matrix elements.

Another system wherein photoexcitation allows access to the transition state region of a bimolecular excited state reaction wherein nonadiabatic effects play an important role is the photoexcitation of H_2S near 200 nm. The conically intersecting $^1A_2$ and $^1B_1$ excited states accessed in the 190-nm absorption band of H_2S mix and split at non-C_{2v} geometries to form a bound excited potential energy surface and an adiabatically dissociative surface. The dissociative adiabat has the general shape of the schematic surface in Figure 1, although it has points of conical intersection (seams if you include the bend) with the bound-potential energy surface. Which state or states is/are reached in the absorption band near 190 to 200 nm is still under question, but photoexcitation does give access to a region near the saddle point on the lower dissociative surface and near the conical intersection between the two adiabats. The numerous experiments on this system have been reviewed in other papers (96–98), but one of the measurements apparently most sensitive to the region of the conical intersection between the surfaces is the emission spectrum from the dissociating molecule (98). Although Heumann & Schinke's recent dynamics calculations are the best to date in addressing the product quantum state distributions and emission features (96, 97), thus far they have relied on an approximate transformation to a diabatic basis currently being investigated by other workers (H-J Werner, personal communication). Although the best approximate "diabatic" basis (92, 93) seeks to separate the Rydberg configuration from the valence ones, the electronic configuration on what they term the "dissociative diabat" changes between two locally repulsive electronic configurations. Such

a change in electronic wavefunction indicates that one has not found a good diabatic representation, although in this system the off-diagonal coupling between the two repulsive configurations may be strong enough that this causes no problem.

While the H_2S system is one of the most tractable both experimentally and theoretically to investigate a nonadiabatic chemical reaction, it exemplifies the pervasive difficulty of finding a good diabatic representation of the Hamiltonian. This problem challenges theory as one tries to include nonadiabatic effects in exact quantum scattering calculations. The electronic structure calculation by definition gives the potential energy surfaces in the adiabatic representation. The difficulty and pitfalls in attempting to transform to an approximately diabatic representation are well known (26, 99); the best work actually calculates derivative coupling matrix elements on the resulting diabats to ensure that they are decent (100). Clearly the best solution to the present uncertainty in the "exact quantum" scattering calculations that rely on an approximate diabatic representation is to calculate the derivative couplings and to do the dynamics calculation in the adiabatic representation (KF Freed, personal communication) with all derivative couplings and geometric phase effects included. Happily, widely used exact quantum scattering methods like the discrete variable representation (DVR) (101a,b) are amenable (JC Light, personal communication) to including derivative couplings so that the scattering calculation may be done without attempting to transform to a diabatic representation. Progress in this area is ongoing, but this author hopes that others in the electronic structure community will join the practitioners who include calculation of derivative coupling matrix elements with their potential energy surfaces. Only with this can we achieve uniformly reliable ab initio predictive ability for multidimensional nonadiabatic systems.

WHERE DYNAMICS ON MULTIDIMENSIONAL POTENTIAL ENERGY SURFACES BECOME NONADIABATIC

Although historically investigators have tried to treat many ground-state chemical reactions within the Born-Oppenheimer approximation, a simple example illustrates that this treatment can fail if the regions of the surface the molecule samples change. If one alters the approach geometry or the collision energy of two reactants, for instance, a reaction that was well approximated as adiabatic may become markedly nonadiabatic. As an example, the chemical reaction $H + O_2 \rightarrow OH + O$ is reasonably well described within the Born-Oppenheimer approximation if one restricts attention to collisions with just barely enough energy to surmount the barrier along the adiabatic reaction coordinate. At these

energies, the molecule does not have enough energy to access the conical intersections at the T-shaped or linear approach geometries characterized by Pack and Walch (102–106; SP Walch, personal communication). However, workers have been tempted to use the adiabatic approximation to model the reaction at a collision energy of 2.4 eV (107a). Then at these energies potentially reactive H atom approach trajectories are not restricted to the Jacobi angle near 50 degrees (characterizing the adiabatic reaction coordinate near the transition state). Indeed, the incoming H atom velocity at a collision energy of 2.4 eV is faster than O_2 rotation, so a substantial fraction of the reactive trajectories with enough energy to reach the HO_2 intermediate will attempt to do so near both linear and T-shaped geometries. At these geometries, the trajectories pass near the conical intersections between the lower and upper adiabats (from the conical intersections between the ^{2}A- and the ^{2}E-states and the $^2A_2$ and $^2B_1$ states), and thus necessarily undergo strongly nonadiabatic dynamics. Recent theoretical work (107b) on a similar system, $O + H_2$, confirms what is anticipated here and in a previous review article (108), that even when the conical intersection is energetically and geometrically remote from the minimum energy reaction path, such nonadiabatic effects can influence the dynamics substantially if the collision energy is high enough to access the conical intersection(s). Furthermore, one must not conclude from this example that only reactions at high collision energies are subject to nonadiabatic effects. In ozone isomerization in the ground state, the transition state is within a few wavenumbers of a conical intersection with the next higher potential energy surface (109, 110). In the bromopropionyl chloride $1^1A''$ dissociation discussed earlier in this review, there is no energetically accessible geometry where the molecule can pass the barrier to C-Br fission adiabatically with unit probability; the avoided crossing is narrowly avoided everywhere the dynamics accesses. The same is true of most long-distance electron transfer reactions (14). Finally, consider the ground state reactions of H + NO. If one lowers the collision energy of the H + NO reactants so they do not have enough energy to encounter the problematic region of the potential energy surface (near the conical intersection) in the entrance channel as they try to surmount the barrier to forming the HNO intermediate, one can still not assume that the reaction will proceed adiabatically. This is because in the O + NH and N + OH exit channels there are regions of the multidimensional energy surface that come energetically close to another adiabat, and the energies of these narrowly avoided crossings are lower than the energy required to surmount the entrance channel barrier (111).

Clearly, researchers need to determine what regions of a multidimensional reactive potential energy surface a molecule samples in order to predict whether nonadiabatic effects play an important role in the reaction rate or dynamics. The

rest of this section details a few experiments that begin to address this issue. In the first example, that of CH_3NH_2, there is an energetically accessible conical intersection on the reactive potential energy surface, but the dynamics is still largely adiabatic because the amplitude of the scattering wavefunction is small near the region of the conical intersection. In the second example, the photodissociation of vibrationally excited CX_3I (X = H,D,F) and ICN, we can decrease the fraction of the dissociative trajectories on the excited state surface that cross near a conical intersection by vibrationally exciting the molecule in the bend prior to photoexcitation; the resulting decrease in branching to the nonadiabatic product channel is substantial. Finally, in two photodissociation experiments, one on HCO and one on OClO, recently performed by other research groups as described below, tuning the excitation laser into different excited state resonances influences whether the scattering wavefunction accesses regions of the potential energy surfaces that are susceptible to nonadiabatic interactions.

How have recent photodissociation experiments elucidated the importance of considering what regions of the potential energy surface the reactive trajectories access in determining whether nonadiabatic effects will be important? In the $\tilde{A}$ state photodissociation of both NH_3 and CH_3NH_2, there is a conical intersection along the N-H and C-N fission reaction coordinates respectively. If the bond fission proceeds adiabatically as the trajectories traverse the conical intersection, excited state NH_2 $\tilde{A}(^2A_1)$ product is formed. Diabatic traversal of the conical intersection results in a transition from the upper to the lower adiabat shown in Figure 14, producing ground state NH_2 product. Because nonadiabatic transitions occur efficiently at conical intersections, one expects a significant fraction of ground-state NH_2 products. However, while N-H fission in ammonia results in a mixture of the two products at energies where both exit channels are energetically allowed (112), C-N fission in CH_3NH_2 produces only excited state NH_2 (113). To understand how the dissociative trajectories manage to traverse the reaction coordinate adiabatically despite the conical intersection, one must consider the detailed dynamics that the molecule undergoes. Upon Franck-Condon excitation to the upper adiabat, where the equilibrium geometry is planar rather than pyramidal about the N atom, NH_2 wagging motion ensues, as evidenced by the structure in the absorption spectrum assigned to a progression in the NH_2 wag in CH_3NH_2 (114). As the molecule traverses the conical intersection with considerable energy in NH_2 wagging motion, the amplitude of the dissociative wavefunction is small at planar geometries and large at bent geometries at the outer turning points of the wagging motion, so there is little amplitude near the point of conical intersection in Figure 14. Classically, then, trajectories traverse the conical intersection mainly at bent geometries where the splitting between the upper and lower adiabats is large and the system thus remains on the upper adiabat throughout the dissociation and results in

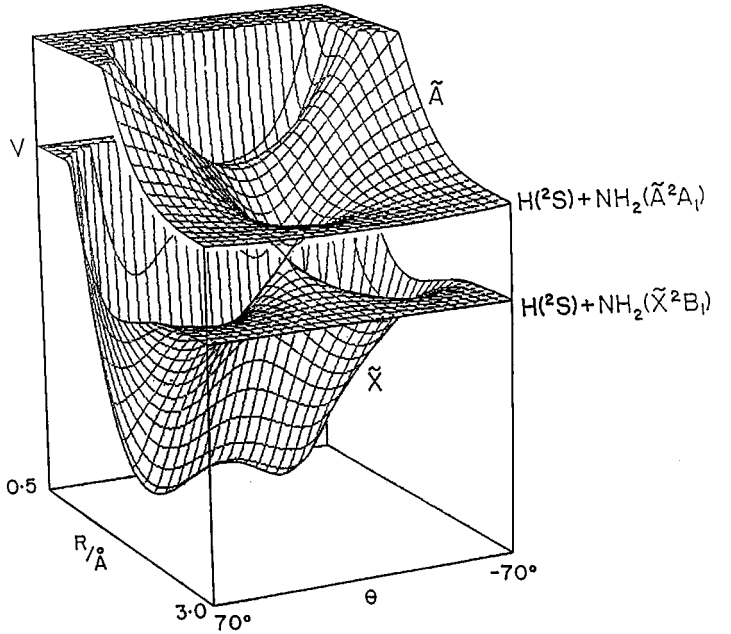

Figure 14 Ground and first excited state potential energy surfaces for ammonia, showing the region of intersection along the N-H bond fission coordinate (or C-N bond fission coordinate in CH_3NH_2) as it varies with the out-of-plane angle θ. (Reproduced with permission from Figure 7 of Reference 112, copyright 1989, American Institute of Physics.)

excited state NH_2 product. Other experiments have sought to control whether the dissociative trajectories traverse the conical intersection at geometries near the point of conical intersection or at bent geometries where the splitting is larger, so as to control the resulting branching between adiabatic and diabatic dissociation products. In CX_3I (X = H,D,F) (115) and ICN (116–118), if one photoexcites molecules with one or more quanta in the bend: the dissociative trajectories traverse the conical intersection at bent geometries where the splitting between adiabats is larger, resulting in an increase in the branching to the adiabatic reaction products. The ab initio prediction of these phenomena (119) is only possible because global potential surfaces with derivative coupling matrix elements have been calculated for the CH_3I and ICN systems (120, 121), a true feat because of the strong spin-orbit coupling as well as the derivative coupling. Decades of earlier theoretical treatments of the $I(^2P_{3/2})$:$I(^2P_{1/2})$ branching in CH_3I neglected to include the e-symmetry bend; they included only the C-I stretch and the a_1 umbrella CH_3 bend; this shows how cautious one must be in

reduced-dimensionality treatments not to neglect the critical nuclear degrees of freedom in the nonadiabatic phenomena.

A somewhat different example of the sensitivity of nonadiabatic effects to the region of the surface accessed by the molecular wavefunction occurs in the photodissociation of HCO. In that system, excited state resonances whose wavefunctions sample linear geometries on the upper of two Renner-Teller coupled surfaces, thus nearing the seam of electronic degeneracy with the lower dissociative surface, evidence much larger widths because of their fast nonadiabatic decay onto the lower Born-Oppenheimer potential energy surface (122–125). Finally, two electronic states important in the indirect photodissociation channels of OClO at wavelengths longer than 400 nm, the 1^2A_1 state and the 1^2B_2 state recently investigated by Peterson & Werner (126), mix and split at non-C_{2v} geometries (thus forming a conical intersection in two degrees of freedom, or an intersection seam in three); this geometry-dependent interaction is intimately tied to the highly selective product branching between $Cl + O_2$ and $ClO + O$ observed by Davis & Lee (127) when they excited into selected resonances in the $\tilde{A}\ ^2A_2$ state, e.g. [500] versus [402], with similar energies but varying numbers of quanta in the antisymmetric stretch.

CONCLUDING REMARKS

The study of nonadiabatic effects in chemical reaction dynamics is one of the most current and active areas of investigation. A talented cadre of young experimentalists is joining the largely theory-oriented group of investigators making progress in this area (128; 129a,b; 130; 131). The experiments described in this review force one to reconsider the conventionally accepted range of validity of the Born-Oppenheimer approximation, one of the most fundamental assumptions in chemical reaction dynamics. They elucidate the critical role nonadiabaticity can play in determining the branching between energetically allowed product channels in bimolecular and unimolecular reactions. They not only demonstrate the importance of considering the possibility of nonadiabaticity at the transition state of any chemical reaction with a barrier along the reaction coordinate, they also begin to identify what classes of chemical reactions are most susceptible to these effects. Progress in many groups continues on not only the gas phase front reviewed here, but also on electronically nonadiabatic processes in condensed phases (132–139). It is the hope of this author that further work in experiment and theory will develop both our ability to achieve an exact quantum prediction for electronically nonadiabatic dynamics and, perhaps more importantly, our intuition for what systems should evidence significant alterations in reaction rates and product branching resulting from a breakdown in the Born-Oppenheimer approximation.

ACKNOWLEDGMENTS

The work described in this review was pursued over the past five years in programs supported individually by the National Science Foundation, under renewal grant number CHE-9619376, and the Division of Chemical Sciences, Office of Basic Energy Sciences, Office of Energy Research, US Department of Energy, under grant DE-FG02-92ER14305. I thank the graduate and undergraduate students who pursued the work reviewed here with me and my ab initio mentors KF Freed, M Head-Gordon, and MM Francl. D Truhlar is acknowledged for helping make this review more scholarly. I thank the accomplished theory/experiment team of Alexander and Dagdigian, whose work first sparked my interest in electronically nonadiabatic processes and GR Fleming, whose support enabled me to continue this work at The University of Chicago.

Literature Cited

1. Laidler KJ, King MC. 1983. *J. Phys. Chem.* 87:2657–64
2. Truhlar DG, Garrett BC, Klippenstein SJ. 1996. *J. Phys. Chem.* 100:12771–93
3. Robinson PJ, Holbrook KA. 1972. *Unimolecular Reactions*. London: Wiley Intersci.
4. Levine RD, Bernstein RB. 1987. *Molecular Reaction Dynamics and Chemical Reactivity*, pp. 276–89. New York: Oxford Univ. Press
5. Bowman JM, Schatz GC. 1995. *Annu. Rev. Phys. Chem.* 46:169–95
6. Truhlar DG, Schwenke DW, Kouri DJ. 1990. *J. Phys. Chem.* 94:7346–52
7. Miller WH. 1990. *Annu. Rev. Phys. Chem.* 41:245–81
8. Miller WH. 1993. *Acc. Chem. Res.* 26: 174–81
9. Ohsaki A, Nakamura H. 1990. *Phys. Rep.* 187:1–62
10. Born M, Oppenheimer R. 1927. *Ann. Phys.* 84:457–84
11. Evans MG, Polanyi M. 1935. *Trans. Faraday Soc.* 31:875–94
12. Evans MG, Polanyi M. 1938. *Trans. Faraday Soc.* 34:11–29
13. Wigner E. 1938. *Trans. Faraday Soc.* 34:29–41
14. Closs GL, Miller JR. 1988. *Science* 240:440–46
15. Salem L. 1982. *Electrons in Chemical Reactions*. New York: Wiley Intersci.
16. Salem L. 1974. *J. Am. Chem. Soc.* 96: 3486–501
17. Tully JC. 1976. In *Dynamics of Molecular Collisions*, Part *B*, ed. WH Miller, pp. 217–67. New York: Plenum
18. Schulz PA, Sudbø AaS, Krajnovich DJ, Kwok HS, Shen YR, Lee YT. 1979. *Annu. Rev. Phys. Chem.* 30:379–409
19. Crim FF. 1984. *Annu. Rev. Phys. Chem.* 35:657–91
20. Uzer T. 1991. *Phys. Rep.* 199:73–146
21. Freed KF, Nitzan A. 1976. In *Energy Storage and Redistribution in Molecules*, ed. J Hinze, pp. 467–91. New York: Plenum
22. Yarkony DR. 1996. *Rev. Mod. Phys.* 68: 985–1013
23. Köppel H, Manthe U. 1992. In *Time-Dependent Quantum Molecular Dynamics*, ed. J Broeckhove, L Lathouwers, pp. 83–95. New York: Plenum
24. Nakamura H. 1991. *Int. Rev. Phys. Chem.* 10:123–88
25. Yarkony DR. 1996. *Rev. Mod. Phys. Chem.* 100:18612–28
26. Garrett BC, Truhlar DG. 1981. In *Theoretical Chemistry: Advances and Perspectives*, ed. D Henderson, 6A:215–89. New York: Academic
27. Garrett BC, Truhlar DG, Melius CF. 1983. In *Energy Storage and Redistribution in Molecules*, ed. J Hinze, pp. 375–95. New York: Plenum
28. Tawa GJ, Mielke SL, Truhlar DG,

Schwenke DW. 1994. In *Advances in Molecular Vibrations and Collision Dynamics: Quantum Reactive Scattering*, ed. JM Bowman, 2B:45–116. Greenwich, CT: JAI
29. Baer M. 1983. In *Molecular Collison Dynamics*, ed. JM Bowman, pp. 117–55. Berlin: Springer-Verlag
30. Sidis V. 1992. *Adv. Chem. Phys.* 82:73–134
31. Chapman S. 1992. *Adv. Chem. Phys.* 82:423–83
32. Nakamura H, Zhu C. 1996. *Comments At. Mol. Phys.* 32:249–66
33. Tully JC. 1991. *Int. J. Quant. Chem. Symp.* 25:299–309
34. Nakamura H. 1996. In *Dynamics of Molecules and Chemical Reactions*, ed. RE Wyatt, JZH Zhang, pp. 473–529. New York: Dekker
35. Dagdigian PJ. 1997. *Annu. Rev. Phys. Chem.* 48:95–123
36. Whetten RL, Ezra GS, Grant ER. 1985. *Annu. Rev. Phys.Chem.* 36:277–320
37. Domcke W, Stock G. 1997. *Adv. Chem. Phys.* 100:1–169
38. Koeppel H, Domcke W. 1997. In *Encyclopedia in Computational Chemistry*, ed. P von Schleyer. New York: Wiley
39. Koeppel H. 1997. *Z. Phys. Chem.* 200:3–10
40. Berry MV. 1984. *Proc. R. Soc. London Ser. A* 392:45–57
41. Shapere A, Wilczek F. 1989. *Geometric Phases in Physics*. Singapore: World Sci.
42. Mead CA. 1992. *Rev. Mod. Phys.* 64:51–85
43. Zwanziger JW, Koenig M, Pines A. 1990. *Annu. Rev. Phys. Chem.* 41:601–46
44. Kuppermann A. 1996. In *Dynamics of Molecules and Chemical Reactions*, ed. RE Wyatt, JZH Zhang, pp. 411–72. New York: Dekker
45. Frisch MJ, Trucks GW, Head-Gordon M, Gill PMW, Wong MW, et al. 1992. *GAUSSIAN 92 Rev. C*. Pittsburgh: Gaussian Inc.
46. Shaik SS. 1981. *J. Am. Chem. Soc.* 103: 3692–701
47. Silver DM. 1974. *J. Am. Chem. Soc.* 96: 5959–67
48. Michl J, Bonačić-Koutecký V. 1990. *Electronic Aspects of Organic Photochemistry*, p. 20, 276. New York: Wiley
49. Evans AG, Evans MG. 1935. *Trans. Faraday Soc.* 31:1400–10
50. Wynne-Jones WFK, Eyring H. 1935. *J. Chem. Phys.* 3:492–505
51. Person MD, Kash PW, Schofield SA, Butler LJ. 1991. *J. Chem. Phys.* 95: 3843–46
52. Person MD, Kash PW, Butler LJ. 1992. *J. Chem. Phys.* 97:355–73
53. Kash PW, Waschewsky GCG, Butler LJ. 1994. *J. Chem. Phys.* 100:4017–18
54. Manaa MR, Yarkony DR. 1993. *J. Chem. Phys.* 99:5251–56
55. Yarkony DR. 1994. *J. Chem. Phys.* 100: 3639–44
56. Waschewsky GCG, Kash PW, Myers TL, Kitchen DC, Butler LJ. 1994. *J. Chem. Soc. Faraday Trans.* 90:1581–98
57. Kash PW, Waschewsky GCG, Butler LJ, Francl MM. 1993. *J. Chem. Phys.* 99:4479–94
58a. Woodward RB, Hoffmann R. 1970. *The Conservation of Orbital Symmetry*, p. 20. Weinheim: VCH
58b. Carr RV, Kim B, McVey JK, Yang NC, Gerhartz W, Michl J. 1976. *Chem. Phys. Lett.* 39:57–60
58c. Yang NC, Chen M-J, Chen P. 1984. *J. Am. Chem. Soc.* 106:7310–15
59. Kash PW, Waschewsky GCG, Morss RE, Butler LJ, Francl MM. 1994. *J. Chem. Phys.* 100:3463–75
60. Kitchen DC. 1996. *Branching between allowed product channels: acrylic acid photolysis, determining absolute branching ratios, and simple ab initio calculations*. PhD thesis. Univ. Chicago. 132 pp.
61. Myers TL, Kitchen DC, Hu B, Butler LJ. 1996. *J. Chem. Phys.* 104:5446–56 and Erratum *J. Chem. Phys*. 105:2948
62. Browning PW, Kitchen DC, Arendt MF, Butler LJ. 1996. *J. Phys. Chem.* 100: 7765–71
63. Tonokura K, Daniels LB, Suzuki T, Yamashita K. 1997. *J. Phys. Chem. A* 101: 7754–64
64. Kawasaki M, Kasatani K, Sato H, Shinohara H, Nishi N. 1984. *Chem. Phys.* 88:135–42
65. Mo Y, Tonokura K, Matsumi Y, Kawasaki M, Sato T, et al. 1992. *J. Chem. Phys.* 97:4815–26
66. Huang YB, Yang Y-a, He G-x, Gordon RJ. 1993. *J. Chem. Phys.* 99:2752–59
67a. Umemoto M, Seki K, Shinohara H, Nagashima U, Nishi N, et al. 1985. *J. Chem. Phys.* 83:1657–66
67b. Morrison H, Singh TV, de Cardinas L, Severance D. 1986. *J. Am. Chem. Soc.* 108:3862–63
68. Post AJ, Nash JJ, Love DE, Jordan KD, Morrison H. 1995. *J. Am. Chem. Soc.* 117:4930–35

69. Nash JJ, Carlson DV, Kasper AM, Love DE, Jordan KD, Morrison H. 1993. *J. Am. Chem. Soc.* 115:8969–79
70. Deleted in proof
71a. Myers TL, Forde NR, Hu B, Kitchen DC, Butler LJ. 1997. *J. Chem. Phys.* 107: 5361–73
71b. Forde NR, Myers TL, Butler LJ. 1997. *Faraday Discuss. Chem. Soc.* 108:221–42
72. Schiffman A, Nelson DD Jr, Nesbitt DJ. 1993. *J. Chem. Phys.* 98:6935–46
73. Felder P, Yang XF, Huber JR. 1993. *Chem. Phys. Lett.* 215:221–27
74. Kenner R, Rohrer F, Papenbrock T, Stuhl F. 1986. *J. Phys. Chem.* 90:1294–99
75. Yeh P-Y, Leu G-H, Lee Y-P, Chen I-C. 1995. *J. Chem. Phys.* 103:4879–86
76. Leu G-H, Hwang C-W, Chen I-C. 1996. *Chem. Phys. Lett.* 257:481–86
77. Jacobs A, Kleinermanns K, Kuge H, Wolfrum J. 1983. *J. Chem. Phys.* 79: 3162–63
78. Bai YY, Segal GA. 1990. *J. Chem. Phys.* 92:7479–83
79. Harris LE. 1973. *J. Chem. Phys.* 58: 5615–26
80. Graña AM, Lee TJ, Head-Gordon M. 1995. *J. Chem. Phys.* 99:3493–502
81. Ruoff RS, Klots TD, Emilsson T, Gutowsky HS. 1990. *J. Chem. Phys.* 93: 3142–50
82. Wagner PJ, Waite CI. 1995. *J. Phys. Chem.* 99:7388–94
83. Simons J. 1983. *Energetic Principles of Chemical Reactions*. Boston: Jones & Bartlett
84. Zimmerman HE. 1966. *J. Am. Chem. Soc.* 88:1566–67
85. Michl J. 1972. *Mol. Photochem.*, 4:243–86, 257–314
86. Michl J. 1975. *Pure Appl. Chem.* 41: 507–34
87. Michl J. 1974. *Top. Curr. Chem.* 46:1–59
88. Mielke SL, Tawa GJ, Truhlar DG, Schwenke DW. 1993. *J. Am. Chem. Soc.* 115:6436–37
89. Bernardi F, Olivucci M, Michl J, Robb MA. 1996. *Spectrum* 9:1–6
90. Jensen E, Keller JS, Waschewsky GCG, Stevens JE, Graham RL, et al. 1993. *J. Chem. Phys.* 98:2882–90
91. Keller JS, Kash PW, Jensen E, Butler LJ. 1992. *J. Chem. Phys.* 96:4324–29
92. Vaghjiani GL. 1993. *J. Chem. Phys.* 99: 5936–43
93. Stevens RE, Kittrell C, Kinsey JL. 1995. *J. Phys. Chem.* 99:11067–73
94. Stevens JE, Jang HW, Butler LJ, Light JC. 1995. *J. Chem. Phys.* 102:7059–69
95. Stevens JE, Freed KF, Arendt MF, Graham RL. 1994. *J. Chem. Phys.* 101: 4832–41
96. Heumann B, Weide K, Düren R, Schinke R. 1993. *J. Chem. Phys.* 98:5508–25
97. Heumann B, Schinke R. 1994. *J. Chem. Phys.* 101:7488–99
98. Browning PW, Jensen E, Waschewsky GCG, Tate MR, Butler LJ. 1994. *J. Chem. Phys.* 101:5652–64
99. Mead CA, Truhlar DG. 1982. *J. Chem. Phys.* 77:6090–98
100. Hirsch G, Buenker RJ. 1990. *Mol. Phys.* 70:835–48
101a. Lill JV, Parker GA, Light JC. 1982. *Chem. Phys. Lett.* 89:483–89
101b. Light JC, Whitnell RM, Park TJ, Choi SE. 1989. In *Supercomputer Algorithms for Reactivity, Dynamics, and Kinetics of Small Molecules*, ed. A Lagana, *NATO ASI Ser. C*, Vol. 277. Dordrecht: Kluwer
102. Kendrick B, Pack RT. 1995. *J. Chem. Phys.* 102:1994–2012
103. Walch SP, Rohlfing CM, Melius CF, Bauschlicher CW. 1988. *J. Chem. Phys.* 88:6273–81
104. Walch SP, Rohlfing CM. 1989. *J. Chem. Phys.* 91:2373–75
105. Walch SP, Duchovic RJ. 1991. *J. Chem. Phys.* 94:7068–75
106. Walch SP, Duchovic RJ. 1992. Erratum. *J. Chem. Phys.* 96:4050
107a. Kim HL, Wickramaaratchi MA, Zheng XN, Hall GE. 1994. *J. Chem. Phys.* 101:2033–50
107b. Schatz GC, Pederson LA, Kuntz PJ. 1997. *Faraday Discuss. Chem. Soc.* 108:357–74
108. Butler LJ, Neumark DM. 1996. *J. Phys. Chem.* 100:12801–16
109. Xantheas SS, Atchity GJ, Elbert ST, Ruedenberg K. 1991. *J. Chem. Phys.* 94:8054–69
110. Ivanic J, Atchity GJ, Ruedenberg K. 1997. *J. Chem. Phys.* 107:4307–17
111. Guadagnini R, Schatz GC, Walch SP. 1995. *J. Chem. Phys.* 102:784–91
112. Biesner J, Schnieder L, Ahlers G, Xie X, Welge KH, et al. 1989. *J. Chem. Phys.* 91:2901–11
113. Waschewsky GCG, Kitchen DC, Browning PW, Butler LJ. 1995. *J. Phys. Chem.* 99:2635–45
114. Tsuboi M, Hirakawa AY, Kawashima H. 1969. *J. Mol. Spectrosc.* 29:216–29
115. Person MD, Kash PW, Butler LJ. 1991. *J. Chem. Phys.* 94:2557–63
116. Kash PW, Butler LJ. 1992. *J. Chem. Phys.* 96:8923–29

117. Qian J, Tannor DJ, Amatatsu Y, Morokuma K. 1994. *J. Chem. Phys.* 101: 9597–609
118. Bowman JM, Mayrhofer RC, Amatatsu Y. 1994. *J. Chem. Phys.* 101:9469–79
119. Hammerich AD, Manthe U, Kosloff R, Meyer H-D, Cederbaum LS. 1994. *J. Chem. Phys.* 101:5623–46
120. Amatatsu Y, Yabushita S, Morokuma K. 1994. *J. Chem. Phys.* 100:4894–909
121. Amatatsu Y, Morokuma K, Yabushita S. 1991. *J. Chem. Phys.* 94:4858–76
122. Loison J-C, Kable SH, Houston PL. 1991. *J. Chem. Phys.* 94:1796–802
123. Goldfield EM, Gray SK, Harding LB. 1993. *J. Chem. Phys.* 99:5812–27
124. Tanaka K, Davidson ER. 1979. *J. Chem. Phys.* 70:2904–13
125. Dixon RN. 1985. *Mol. Phys.* 54:333–50
126. Peterson KA, Werner H-J. 1996. *J. Chem. Phys.* 105:9823–32
127. Davis HF, Lee YT. 1996. *J. Chem. Phys.* 105:8142–62
128. Ben-Nun M, Levine RD, Jonas DM, Fleming GR. 1995. *Chem. Phys. Lett.* 245:629–38
129a. Cao JY, Loock H-P, Qian CXW. 1994. *J. Chem. Phys.* 101:3395–98
129b. North SW, Mueller J, Hall GE. 1997. *Chem. Phys. Lett.* 276:103–9
130. Kim B, Schick CP, Weber PM. 1995. *J. Chem. Phys.* 103:6903–13
131. Vrakking MJJ, Villeneuve DM, Stolow A. 1996. *J. Chem. Phys.* 105:5647–50
132. Head-Gordon M, Tully JC. 1992. *J. Chem. Phys.* 96:3939–49
133. Head-Gordon M, Tully JC. 1995. *J. Chem. Phys.* 103:10137–45
134. Zadoyan R, Sterling M, Apkarian VA. 1996. *Trans. Faraday Soc.* 92:1821–29
135. Bastista VS, Coker DF. 1997. *J. Chem. Phys.* 106:6923–41, 7102–16
136. Ben-Nun M, Levine RD, Fleming GR. 1996. *J. Chem. Phys.* 105:3035–56
137. Coalson RD, Evans DG, Nitzan A. 1994. *J. Chem. Phys.* 101:436–48
138. Coker DF. 1993. In *Computer Simulation in Chemical Physics*, ed. MP Allen, DJ Tildesley, pp. 315–78. Dordrecht: Kluwer
139. Coker DF, Mei HS, Ryckaert JP. 1998. In *Classical and Quantum Dynamics in Condensed Matter Simulations*, ed. BJ Berne, G Ciccotti, DF Coker. Singapore: World Scientific